THE EUROPEAN
PHYSICAL JOURNAL A

# Hadron physics potential of future high-luminosity B-factories at the $\Upsilon(5S)$ and above

A.G. Drutskoy[1,2,a], F.-K. Guo[3,b], F.J. Llanes-Estrada[4,c], A.V. Nefediev[1,2,5,6,d], and J.M. Torres-Rincon[4,e]

[1] Institute of Theoretical and Experimental Physics, 117218, Moscow, Russia
[2] National Research Nuclear University MEPhI, 115409, Moscow, Russia
[3] Helmholtz-Inst. für Strahlen-und Kernphysik & Bethe Center for Theoretical Physics, Univ. Bonn, D-53115 Bonn, Germany
[4] Depto. Fisica Teorica I, Universidad Complutense Madrid, 28040 Madrid, Spain
[5] Moscow Institute of Physics and Technology, 141700, Dolgoprudny, Moscow Region, Russia
[6] All-Russia Research Institute of Automatics (VNIIA), 127055, Moscow, Russia

**Abstract.** We point out the physics opportunities of future high-luminosity $B$-factories at the $\Upsilon(5S)$ resonance and above. Currently the two $B$-factories, the SuperB factory in Tor Vergata, Italy and the Belle II factory in KEK, Japan, are under development and are expected to start operation in 2017 and 2016, respectively. In this paper we discuss numerous interesting investigations, which can be performed in the $e^+e^-$ center-of-mass energy region from the $\Upsilon(5S)$ and up to 11.5 GeV, where an efficient data taking operation should be possible with the planned $B$-factories. These studies include abundant $B_s$ production and decay properties; independent confirmation and, if found, exhaustive exploration of Belle's claimed charged bottomonia; clarification of puzzles of interquarkonium dipion transitions; extraction of the light-quark mass ratio from hadronic $\Upsilon(5S)$ decays; analysis of quarkonium and exotic internal structure from open flavour decays, leading to severe $SU(3)$ symmetry violations; clarification of whether a hybrid state has similar mass to the $\Upsilon(5S)$ bottomonium, making it a double state; searches for molecular/tetraquark states that should be more stable with heavy quarks; completion of the table of positive-parity $B_J$ mesons and study of their basic properties; production of $\Lambda_b\bar{\Lambda}_b$ heavy baryon pairs, that, following weak decay, open vistas on the charmed baryon spectrum and new channels to study $CP$ violation; confirmation or refutation of the deviation from pQCD of the pion transition form factor, by extending the $Q^2$ reach of current analysis; and possibly reaching the threshold for the production of triply charmed baryons. If, in addition, the future colliders can be later upgraded to 12.5 GeV, then the possibility of copious production of $B_c\bar{B}_c$ pairs opens, entailing new studies of $CP$ violation and improved, independent tests of the CKM picture (through determination of $V_{bc}$), and of effective theories for heavy quarks.

## Contents

[a] e-mail: Drutskoy@itep.ru
[b] e-mail: fkguo@hiskp.uni-bonn.de
[c] e-mail: fllanes@ucm.es
[d] e-mail: nefediev@itep.ru
[e] e-mail: j.torres@fis.ucm.es

# 1 Introduction

In the last years we have witnessed a renaissance of hadron spectroscopy caused by a series of discoveries made at $B$-factories. Before $B$-factories, most of the known states in the spectrum of charmonium and bottomonium lay below the open-flavour thresholds, a well-developed phenomenology based on potential quark models was quite successful in describing properties of these states, and, in particular, threshold effects could be cast into constant mass shifts. However the situation changed dramatically after $B$-factories started operation and data collection. A lot of new states were observed, the majority of them lying above the open-flavour thresholds in the spectra of both charmonium and bottomonium. Many such states in fact are close to various thresholds, so that the threshold effects appear to be the dominant feature, and a drastic departure from the Breit-Wigner form in line shapes is expected, especially when the coupling to the corresponding open-flavour channels is in an $S$-wave. At the same time, a lot of theoretical ideas were put forward to explain the data. As a result, while some experimental observations remain not yet well understood theoretically, a large number of theoretical predictions do call for improvements in the experimental situation, which are expected to be achieved at the next-generation $B$-factories, such as SuperB and Belle II.

This paper is mostly devoted to the heavy quarkonium studies at the centre-of-mass energy above the $\Upsilon(4S)$. We will review available experimental results and different theoretical models applicable in the heavy quarkonium physics with a significant emphasis on unresolved theoretical issues. The potentially important experimental studies in this area, feasible for the future high-luminosity $B$-factories, will also be discussed. In particular, the SuperB experiment plans to collect during several years of running about $75\,\mathrm{ab}^{-1}$ at the $\Upsilon(4S)$ and a few $\mathrm{ab}^{-1}$ at the $\Upsilon(5S)$ and, probably, at the $\Upsilon(6S)$ and around. With expected integrated luminosity significantly larger than previously available at $B$-factories, such experiment will become a valuable source of experimental data which not only will allow to improve statistics for previously studied reactions, but it will enable to study various rare decays and reactions, not achievable at present.

A large part of our discussion will be the isoscalar vector hidden-bottom state that resides in this region, with mass and width, according to recent measurements [1],

$$M = 10876 \pm 2\,\mathrm{MeV},$$
$$\Gamma = 43 \pm 4\,\mathrm{MeV}. \tag{1}$$

In the framework of the quark model, this state is a conventional $n^{2S+1}L_J = 5^3S_1\ b\bar{b}$ meson, where $n$ is the radial quantum number, while $S$, $L$, and $J$ denote the quark spin, the quark-antiquark angular momentum, and the total spin, respectively[1]. In what follows we therefore refer to the corresponding state as $\Upsilon(5S)$. However, we discuss

---

[1] $S$-$D$–wave mixing is discussed below in sects. 2.5 and 5.2.

in addition other possible non-$b\bar{b}$ vector resonances residing in this energy region.

We will then extend the discussion to larger energies, particularly the $\Upsilon(6S)$ resonance, but also several interesting thresholds expected above it. To keep the review within a manageable size we have limited ourselves to brief comments on most of the topics. We hope that the references given will be a reasonable starting point for the interested reader.

Measurements that can be mostly conducted at the $\Upsilon(4S)$, and much of the flavour discussion involving $B_s$ decays, have been the object of other studies and different theoretical approaches, so we have purposefully avoided dwelling on them here. We have included some discussion on quarkonium states, but the reader may want to refer to the quarkonium working group report [2] for extended coverage of many topics.

# 2 Closed-flavour analysis at $\Upsilon$(5S)

## 2.1 Dipion transitions from $\Upsilon$(5S)

The $\Upsilon(5S)$, well above open-bottom threshold, decays mainly to open-flavour channels. Closed-flavour decays are however also easily observable, and those with the largest branching fractions are dipion transitions into other bottomonium states. They are an important source of information on the nature of this state. Two types of dipion transitions can be identified: transitions without spin flip ($\Upsilon(5S) \to \Upsilon(nS)\pi\pi$ with $n < 5$) and transitions with spin flip ($\Upsilon(5S) \to h_b(nP)\pi\pi$ with $n = 1, 2$).

### 2.1.1 Dipion transitions without $b$-quark spin flip

Dipion transitions $e^+e^- \to \Upsilon(nS)\pi^+\pi^-$ with $n = 1, 2, 3$ measured by Belle [3] peak at the same centre-of-mass energy (see fig. 1),

$$\mu = [10888.4^{+2.7}_{-2.6} \pm 1.2]\,\mathrm{MeV},$$
$$\Gamma = [30.7^{+8.3}_{-7.0} \pm 3.1]\,\mathrm{MeV}, \tag{2}$$

and the deviation of this quantity (more than $2\sigma$) from the maximum position in the hadronic cross-section (vertical dashed line in fig. 1) has been discussed theoretically assuming different interpretations. In particular, $B^{(*)}\text{-}\bar{B}^{(*)}$ rescattering was suggested in [4] as a possible mechanism responsible for the peak shift in the $\Upsilon(nS)\pi^+\pi^-$ dipion invariant-mass distribution.

Another interesting feature of the distribution shown in fig. 1 is an almost zero cross-section level outside the $\Upsilon(5S)$ resonance region. It indicates that the $\Upsilon(nS)\pi^+\pi^-$ states cannot be produced in the continuum, but only through the resonance formation mechanism. In contrast, the $b\bar{b}$ production cross-section level is rather high at all energies below the $B\bar{B}$ mass threshold. This difference remains to be explained theoretically. Measurements
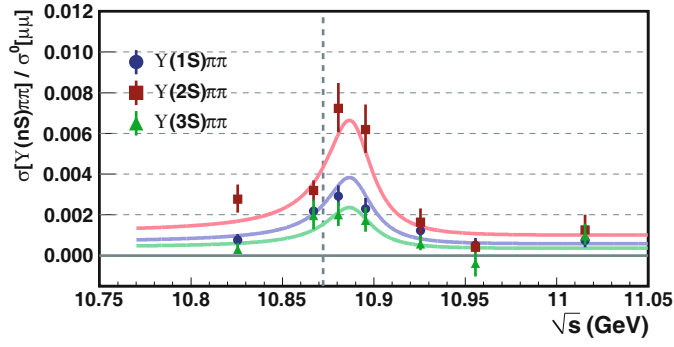
**Fig. 1.** The ratio $\sigma[e^+e^- \to \Upsilon(nS)\pi^+\pi^-]/\sigma[e^+e^- \to \mu^+\mu^-]$ for $n = 1, 2, 3$, as measured by Belle [3]. The vertical dashed line marks the position of the inclusive hadronic cross-section maximum.

of the $B^*\bar{B}^*$ exclusive channel cross-section as a function of the centre-of-mass energy may shed some light on this difference as well as on the mass deviation discussed above.

Furthermore, Belle reported [5] observation of an unexpectedly large $\Upsilon(nS)\pi^+\pi^-$ ($n = 1, 2, 3$) production at the $\Upsilon(5S)$ energy comparing with one at the $\Upsilon(4S)$. In particular, the measured values,

$$\Gamma[\Upsilon(5S) \to \Upsilon(1S)\pi^+\pi^-] = [0.59 \pm 0.04 \pm 0.09]\,\text{MeV},$$

$$\Gamma[\Upsilon(5S) \to \Upsilon(2S)\pi^+\pi^-] = [0.85 \pm 0.07 \pm 0.16]\,\text{MeV},$$

$$\Gamma[\Upsilon(5S) \to \Upsilon(3S)\pi^+\pi^-] = [0.52^{+0.20}_{-0.17} \pm 0.10]\,\text{MeV}, \quad (3)$$

appear to be by about two orders of magnitude larger than similar dipion decays of $\Upsilon(nS)$, with $n < 4^2$. A tetraquark explanation of such an anomalous production suggests that the final states are produced from a tetraquark with a mass of 10890 MeV, rather than from the $\Upsilon(5S)$ [11, 12]. Another possible mechanism is related to strong interference between the direct production and the final-state interactions [13,14].

Another question related to the dipion transitions from $\Upsilon(nS)$ states is the shape of the dipion invariant-mass spectrum. Before the observation of the $\Upsilon(4S)$ and $\Upsilon(5S)$ dipion decays, there was a question about the peculiar dipion invariant-mass spectrum of the $\Upsilon(3S) \to \Upsilon(1S)\pi^+\pi^-$ transition [7,15]. In analogous heavy quarkonium transitions, such as $\psi' \to J/\psi\pi^+\pi^-$ and $\Upsilon(2S) \to \Upsilon(1S)\pi^+\pi^-$, the $\pi^+\pi^-$ invariant-mass distribution shows a single broad peak towards the higher end of the phase space (see, for example, the upper plot in fig. 2). In the $\Upsilon(3S) \to \Upsilon(1S)\pi^+\pi^-$ transition, however, the structure is quite different, with two bumps showing up (the middle plot in fig. 2). Similar double-bump structures were observed later in higher $\Upsilon(nS)$ dipion transitions (see figs. 3 and 4). In particular, the $\pi^+\pi^-$ invariant-mass distribution for the
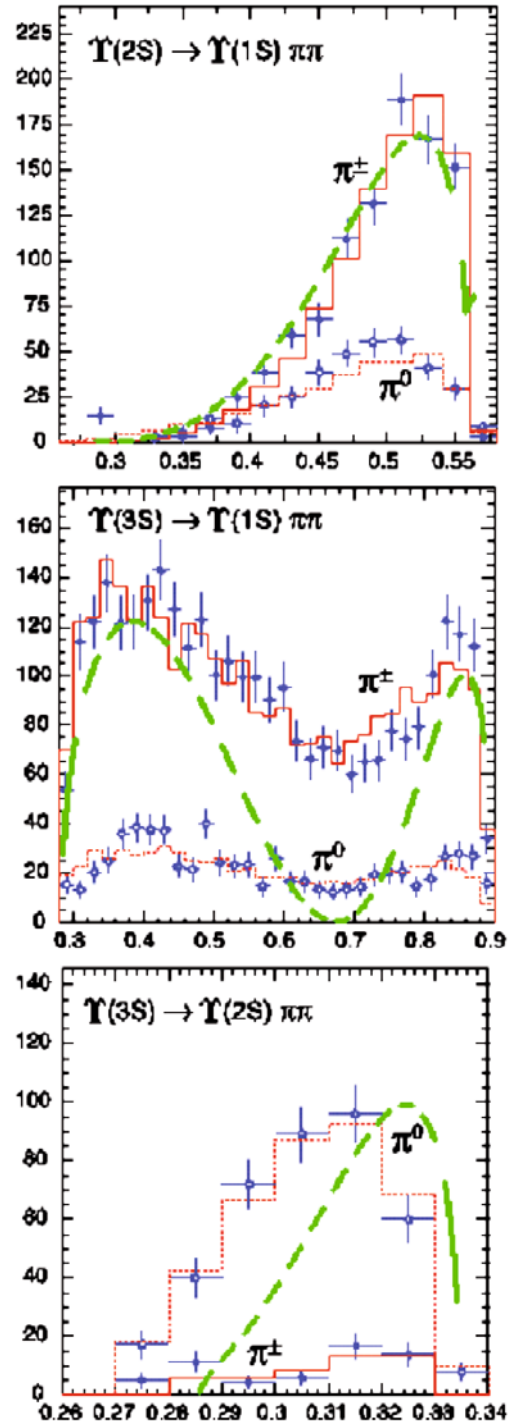


**Fig. 2.** CLEO Collaboration data for dipion transitions from $\Upsilon(2S)$ and $\Upsilon(3S)$ states [7]. Theoretical results from [10] are shown with the dashed green line.

$\Upsilon(4S) \to \Upsilon(1S)\pi^+\pi^-$ transition was measured first by the Belle Collaboration [16], and later on by the BaBar Collaboration, together with the $\Upsilon(4S) \to \Upsilon(2S)\pi^+\pi^-$ [8]. Finally, measurements of the $\Upsilon(5S) \to \Upsilon(nS)\pi^+\pi^-$ transitions, with $n < 4$, were reported by the Belle Collaboration [5,17,18].

---

2 Typical values of the widths for the decays $\Upsilon(nS) \to \Upsilon(n'S)\pi^+\pi^-$, with $n' < n < 4$, appear to be of order a few keV [6–8], in agreement with theoretical predictions [9,10].
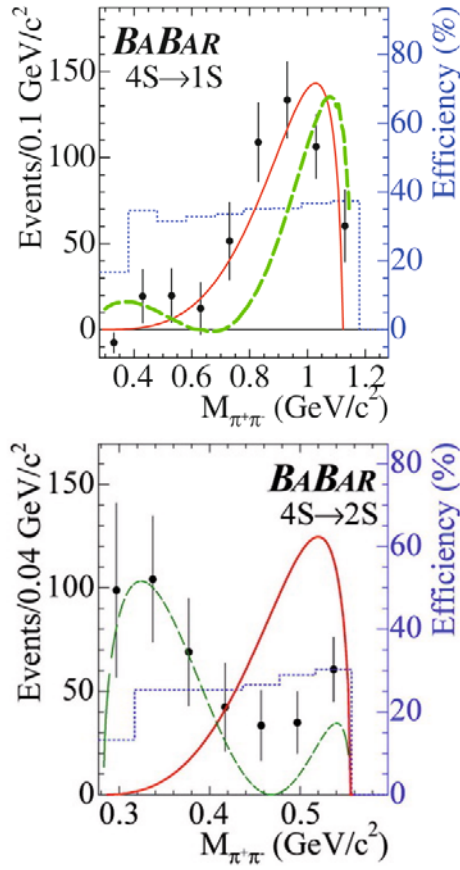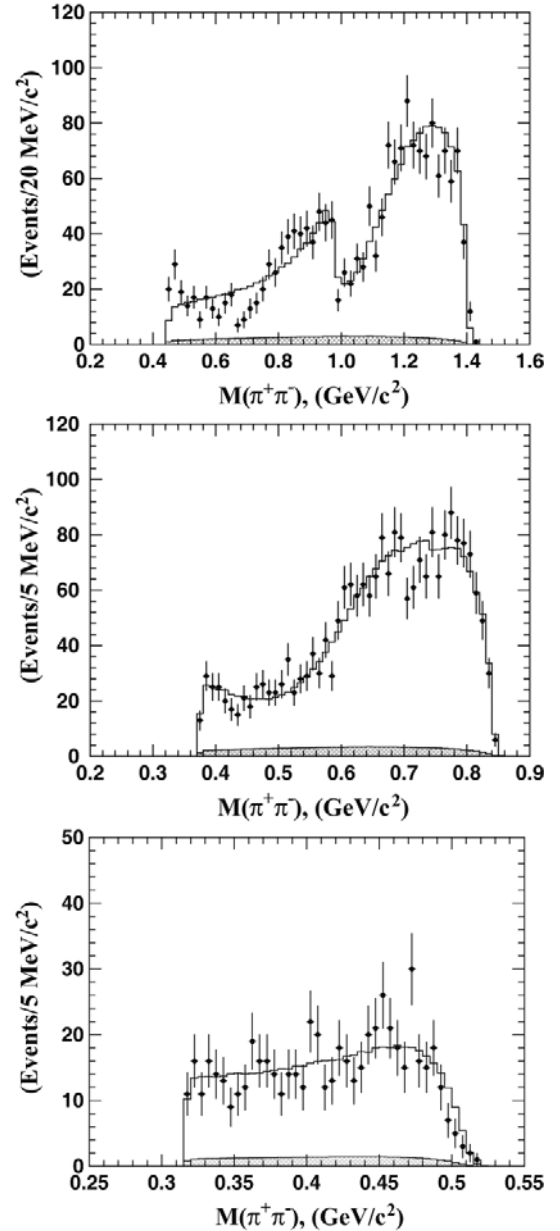
**Fig. 3.** BABAR Collaboration data for dipion transitions from $\Upsilon(4S)$ state [8]. Theoretical results from [10] are shown with the dashed green line.

Compounding this problem, one should notice that the kinematically allowed phase space is quite different in various transitions. For $\Upsilon(2S) \to \Upsilon(1S)\pi^+\pi^-$, the dipion invariant mass is limited up to about 560 MeV, similarly to the analogous charmonium transition $\psi(2S) \to J/\psi\pi^+\pi^-$. On the other hand, most of the transitions having a more complicated dipion invariant-mass distribution have larger phase space, with the exception of the $\Upsilon(4S) \to \Upsilon(2S)\pi^+\pi^-$.

From the theory point of view, these double-peak structures were studied by a number of authors, for reviews, see [19–21]. The problem was further investigated in recent years (see, for example, [9,10,22]). Among various explanations, it is interesting to notice the proposal of an isovector exotic $b\bar{b}q\bar{q}$ state in the bottomonium mass region [21,23,24].

A small bump close to the lower end of the mass distribution in the $\Upsilon(4S) \to \Upsilon(1S)\pi^+\pi^-$ was noticed in [25]. There has been no agreement whether the $S$-wave $\pi\pi$ final-state interaction (in agreement with the strong $f_0(500)$ (or $\sigma$) signal in the reaction $J/\psi \to \omega\pi\pi$ [26]), or rather a relativistic correction, is the key to understanding the structure in the region 400–600 MeV.

When the emitted pions are soft, an effective chiral Lagrangian can be used, with first steps taken already at the time of the charm discovery [27]. At lowest order each



**Fig. 4.** Belle Collaboration data for dipion transitions from $\Upsilon(5S)$ state to $\Upsilon(1S)\pi^+\pi^-$ (upper plot), $\Upsilon(2S)\pi^+\pi^-$ (middle plot), and $\Upsilon(3S)\pi^+\pi^-$ (lower plot) [17,18].

$\Upsilon(n) \to \Upsilon(m)\pi\pi$ channel requires four unknown parameters [28] that cannot be measured elsewhere, so that the predictive power is very limited.

Another issue is the importance of open-bottom coupled channels [29–31]. They cannot be simply neglected in the effective field theory, because the gap between heavy quarkonium and open-flavour heavy meson thresholds is often small compared with the hard scale of 1 GeV. Assuming these thresholds are more important than the contact terms described by the chiral Lagrangian[3], one may construct a predictive formalism.

---

[3] This could be checked using the non-relativistic effective field theory proposed in [32,33].
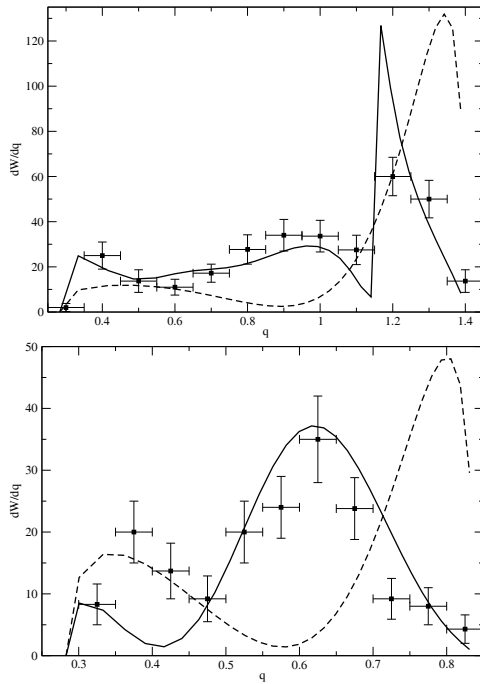
**Fig. 5.** The dipion invariant-mass spectrum for the decays $\Upsilon(5S) \rightarrow \Upsilon(nS)\pi^+\pi^-$ with $n = 1, 2$ ($\Gamma_{\pi^+\pi^-} = \int(\mathrm{d}w/\mathrm{d}q)\mathrm{d}q$, $q \equiv M_{\pi^+\pi^-}$). Data are from [5], while theoretical curves are from [9]. The solid line corresponds to the FSI taken into account properly.



**Fig. 6.** The angular distributions $\mathrm{d}w/\mathrm{d}\cos\theta$ for the transitions $\Upsilon(5S) \rightarrow \Upsilon(1S)\pi^+\pi^-$ (upper plot) and $\Upsilon(5S) \rightarrow \Upsilon(2S)\pi^+\pi^-$ (adapted from [9]) compared to the data from [5]. Theoretical predictions are given without FSI (dashed line) and with FSI (solid line) included.
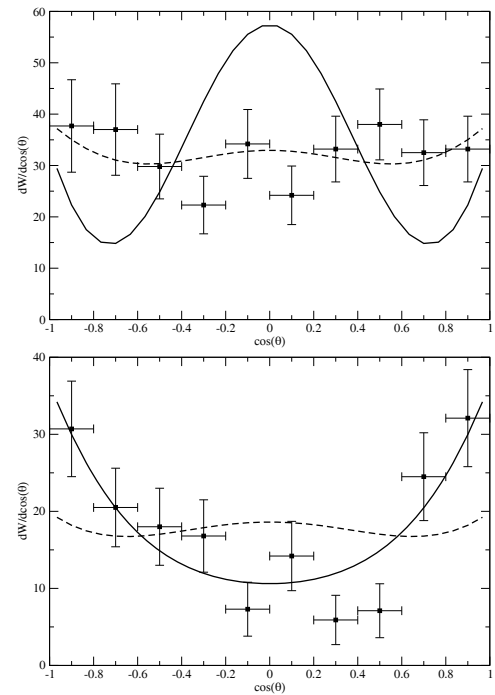
In fact, theorists have provided [9,10] a parameter-free description of the dipion spectra stressing the role of the Adler Zero Requirement (AZR) imposed on the amplitude, as well as that of the Final-State Interaction (FSI). Predictions of the approach [9,10] are shown in figs. 2 and 3 with the green dashed line, as well as in fig. 5. In particular, dips in the $\pi^+\pi^-$ spectrum are explained by the AZR which suppresses the corresponding amplitude at small pion momenta. In the meantime, the peak structure at the lower end of the dipion invariant-mass spectrum (see fig. 5) is explained in [9] to be due to an interplay of the FSI and AZR. Then the angular distributions $\mathrm{d}w/\mathrm{d}\cos\theta$ ($\theta$ is the angle between the initial $\Upsilon$ and the $\pi^+$) are presented in [9,10] for various $\Upsilon(nS) \rightarrow \Upsilon(n'S)\pi^+\pi^-$ transitions and are compared with the data from [5,7] (see fig. 6).

In addition, three-dimensional plots for the differential decay probability $\mathrm{d}w/(\mathrm{d}x\mathrm{d}\cos\theta)$ for various dipion $\Upsilon(nS) \rightarrow \Upsilon(n'S)\pi^+\pi^-$ decays were suggested and presented in [10] (see examples shown in fig. 7), where the dimensionless variable $x \in [0, 1]$ is defined as

$$x = \frac{M_{\pi^+\pi^-}^2 - 4m_\pi^2}{[M(\Upsilon(nS)) - M(\Upsilon(n'S))]^2 - 4m_\pi^2}.$$

While general features of the data have been correctly captured, there remain details to be understood. In the middle panel of fig. 2, the dip predicted in the $\Upsilon(3S) \rightarrow \Upsilon(1S)\pi\pi$ is deeper than experimental data. A similar result was also found in the effective Lagrangian

formalism taking into account the $\pi\pi$ FSI [21], where the dip was made consistent with the data with the help of an additional theorised isovector $b\bar{b}q\bar{q}$ state. Indeed two exotic isovector structures $Z_b(10610)^\pm$ and $Z_b(10650)^\pm$ have been reported in $\Upsilon(5S)$ decays, see sect. 2.2, in all of the $\Upsilon(1S)\pi$, $\Upsilon(2S)\pi$ and $\Upsilon(3S)\pi$ dipion modes. It is important therefore to revisit the lower $\Upsilon$ transitions, including now the effect of possible $Z_b$ states, and to perform a systematic study of all the data for $\Upsilon(nS) \rightarrow \Upsilon(mS)\pi^+\pi^-$ transitions to understand the true mechanism of these decays.

Experimentally, it would be very helpful to measure the dipion and also the $\Upsilon(nS)\pi$ invariant-mass distributions in the $\Upsilon(5S) \rightarrow \Upsilon(nS)\pi^+\pi^-$ precisely, so that one can extract the information of coupling of the $Z_b$ states to the $\Upsilon(nS)\pi$. The information can then be fed back to the lower $\Upsilon(nS)$ dipion transitions, eventually providing a deeper understanding of these puzzling decays.

The future high-luminosity $B$-factories could contribute more precise data on the lower end of the $\pi^+\pi^-$ mass distribution, where Belle data are somewhat insufficient, in order to observe these non-trivial structures in the $\Upsilon(5S)$ dipion transitions. Moreover, this is also a region where the more "normal" dipion transitions such as the $\Upsilon(2S) \rightarrow \Upsilon(1S)\pi^+\pi^-$ show striking differences with the "abnormal" ones like the $\Upsilon(3S) \rightarrow \Upsilon(1S)\pi^+\pi^-$: the lower end is rather suppressed for the former while it is enhanced for the latter.

Next, particular attention should be paid to the region around $1\,\text{GeV}$ (in $\Upsilon(1S)\pi^+\pi^-$ since the other final states
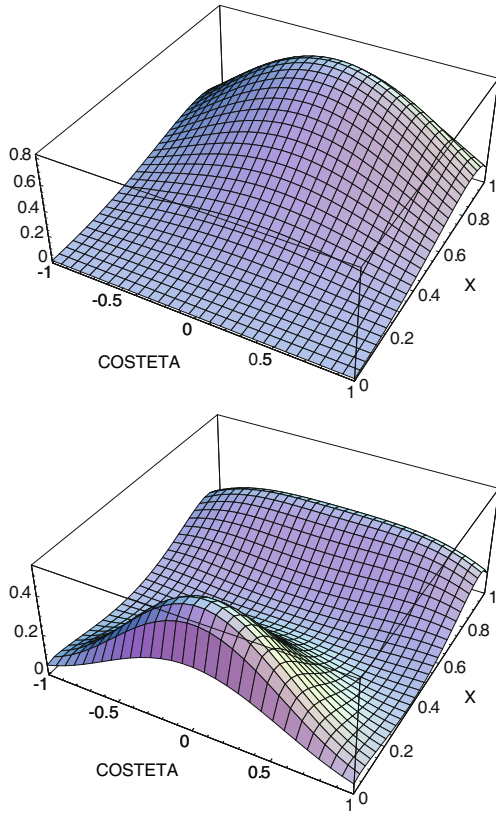
**Fig. 7.** The differential decay probability $\mathrm{d}w/(\mathrm{d}x\mathrm{d}\cos\theta)$ for the transitions $\Upsilon(2S) \to \Upsilon(1S)\pi^+\pi^-$ (upper plot) and $\Upsilon(3S) \to \Upsilon(1S)\pi^+\pi^-$ (adapted from [10]). Further examples can be found in [10].

do not have enough phase space). Detailed knowledge in this 1 GeV region would be helpful in understanding the nature of both the $\Upsilon(5S)$ and the light scalar $f_0(980)$. The transition $\Upsilon(5S) \to \Upsilon(1S)\pi^+\pi^-$ offers a rather unique possibility for studying light scalar mesons in the sense that both the initial and final particles (besides the pions) are $SU(3)$ flavour singlet states. In the $SU(3)$ limit, the production couplings should be equal for up, down, and strange flavours. Hence, this transition is able to provide information on the light scalar mesons complementary to those from the decays such as $J/\psi \to \omega\pi^+\pi^-$ and $J/\psi \to \phi\pi^+\pi^-$.

Precise measurements of the $\Upsilon(5S) \to \Upsilon(1S)K^+K^-$ transition in the region near the $K^+K^-$ threshold would also be quite useful, because the $f_0(980)$ couples strongly to two kaons. The rate for this reaction has been found to be about 9 times smaller than the dipion channel, with a partial width of about 0.067 MeV [5].

Additional important information on the dipion transitions can be obtained with a $B$-factory running at the $\Upsilon(6S)$. The decay widths, dipion invariant-mass spectra and angular distributions in the $\Upsilon(6S) \to \Upsilon(nS)\pi^+\pi^-$ transitions, with $n \leq 4$, should be compared to ones obtained at the $\Upsilon(5S)$. Due to its larger mass, the open-beauty mass threshold effects should be smaller than for

the $\Upsilon(5S)$ and contributions from different processes can be somewhat separated.

### 2.1.2 Dipion transitions with $b$-quark spin flip

Nominally, inverting the spin of the heavy quark in a decay is a process suppressed by a factor $\Lambda_{\mathrm{QCD}}/m_b$. Data however do not always make it obvious. There is a recent Belle Collaboration observation of the $h_b(1P)$ and $h_b(2P)$ states produced via $e^+e^- \to h_b(nP)\pi^+\pi^-$ in the $\Upsilon(5S)$ region [34] (with the data sample of $121.4\,\mathrm{fb}^{-1}$ collected near the $\Upsilon(5S)$ peak).

It raises yet another question related to dipion $\Upsilon(5S)$ transitions since the reported ratios,

$$\frac{\Gamma(\Upsilon(5S) \to h_b(1P)\pi^+\pi^-)}{\Gamma(\Upsilon(5S) \to \Upsilon(2S)\pi^+\pi^-)} \approx 0.4,$$

$$\frac{\Gamma(\Upsilon(5S) \to h_b(2P)\pi^+\pi^-)}{\Gamma(\Upsilon(5S) \to \Upsilon(2S)\pi^+\pi^-)} \approx 0.8, \qquad (4)$$

are unexpectedly large. Indeed, while the $b\bar{b}$ pair is in the spin-triplet state in the vectors $\Upsilon(nS)$, it appears to be in spin-singlet state in the axials $h_b(nP)$. This implies that, unlike the $\Upsilon(5S) \to \Upsilon(2S)\pi^+\pi^-$ transition, proceeding without heavy-quark spin flip, naively such a flip must occur in $\Upsilon(5S) \to h_b(nP)\pi^+\pi^-$, so that the amplitude for the latter process is expected to be suppressed by $\Lambda_{\mathrm{QCD}}/m_b$ when compared with that for the former transition.

Summarising this subsection devoted to dipion transitions, it is important to notice that, with the data sample of about $1\,\mathrm{ab}^{-1}$ collected by a future $B$-factory near the $\Upsilon(5S)$, not only high-statistics data will be available for dipion decays with charged pions, but similar decays with two neutral particles (pions and/or $\eta$'s) in the final state should be readily accessible. Yet another piece of critical information can be obtained with a few hundred $\mathrm{fb}^{-1}$ taken at the $\Upsilon(6S)$.

## 2.2 $Z_b$ states

In 2011 the Belle Collaboration announced the first observation of two charged bottomonium-like states, $Z_b(10610)$ and $Z_b'(10650)$, in five different decay channels of $\Upsilon(5S)$ ($\pi^\pm\Upsilon(nS)$, $n = 1, 2, 3$ and $\pi^\pm h_b(mP)$, $m = 1, 2$) [17,18], with averaged masses and widths [18],

$$M_{Z_b} = 10607.2 \pm 2.0\,\mathrm{MeV}, \quad \Gamma_{Z_b} = 18.4 \pm 2.4\,\mathrm{MeV}, \quad (5)$$

$$M_{Z_b'} = 10652.2 \pm 1.5\,\mathrm{MeV}, \quad \Gamma_{Z_b'} = 11.5 \pm 2.2\,\mathrm{MeV}. \quad (6)$$

These structures are produced from, and reconstructed in, conventional $b\bar{b}$ states, so it is natural to assume that they contain a $b\bar{b}$ quark pair. However, for $Z_b$'s being electrically charged, a pure $b\bar{b}$ assignment is discarded. These states are still in want of confirmation by other experiments and their nature is not well understood yet. It is clear however that they provide an excellent test ground for QCD. In particular, these newly

observed states may be relevant for understanding the dipion $\Upsilon(nS)$, in particular $\Upsilon(5S)$, transitions. Given the proximity of the observed $Z_b$ states to two-body thresholds $B\bar{B}^*(10604.5\pm0.4\,\mathrm{MeV})^4$ and $B^*\bar{B}^*(10650.4\pm0.6\,\mathrm{MeV})$, a molecular interpretation of the $Z_b$'s was suggested shortly after the Belle announcement [35]. Although the four-quark interpretation of the $Z_b$'s still requires a theoretical explanation of their large production cross-section at the $\Upsilon(5S)$ energies, this idea immediately motivated many theoretical efforts (see, for example, [36–44]) and a number of predictions were made following this conjecture. Below we discuss them briefly.

If an exact heavy-quark symmetry is assumed (implying the limit $m_b \to \infty$), a proper basis to consider $S$-wave $B^{(*)}\bar{B}^{(*)}$ pairs consists of the direct product of the eigenstates of the spin operators for the heavy-quark pair and the light-quark pair, $S_{b\bar{b}} \otimes S_{q\bar{q}}$, with $S_{b\bar{b}} = 0,1$ and $S_{q\bar{q}} = 0,1$. Then the wave functions of the $Z_b$ states can be represented as [35]

$$
\begin{aligned}
1^+(1^+)\ Z_b' &: \frac{1}{\sqrt{2}}\left(0_{b\bar{b}} \otimes 1_{q\bar{q}} - 1_{b\bar{b}} \otimes 0_{q\bar{q}}\right), \\
1^+(1^+)\ Z_b &: \frac{1}{\sqrt{2}}\left(0_{b\bar{b}} \otimes 1_{q\bar{q}} + 1_{b\bar{b}} \otimes 0_{q\bar{q}}\right),
\end{aligned}
\tag{7}
$$

where, in the first column, the quantum numbers are quoted in the form $I^G(J^P)$ with $I$ and $J$ being the isospin and total spin of the state, and with the superindices denoting its $G$- and $P$-parity, respectively.

This provides a possible explanation for the anomalous ratios (4) as no suppression is expected for the processes proceeding through the $Z_b(Z_b')\pi$ intermediate states, as cascades [35],

$$
\begin{aligned}
\Upsilon(5S) &\to Z_b(Z_b')\pi \to h_b(1P)(h_b(2P))\pi^+\pi^-, \\
\Upsilon(5S) &\to Z_b(Z_b')\pi \to \Upsilon(nS)\pi^+\pi^-,
\end{aligned}
$$

because components with both heavy-quark spin orientations have equal weight in the $Z_b$'s wave functions. Besides that, representation (7) predicts the interference pattern for the amplitudes of the processes proceeding through the $Z_b$ and $Z_b'$. In particular, for the reactions $\Upsilon(5S) \to h_b(nP)\pi^+\pi^-$ ($n = 1, 2$), because of the different relative sign between the two components of the wave function, eq. (7) predicts constructive interference between the $Z_b$ peaks and destructive interference outside this region [35]. In the meantime, the interference pattern is quite opposite for the reactions $\Upsilon(5S) \to \Upsilon(nS)\pi^+\pi^-$. This prediction is consistent with the recent Belle data [18] (small dip between peaks in fig. 8 *versus* a well-pronounced dip between peaks in fig. 9).

Furthermore, it is argued in [14] that results of model calculations both for the dipion invariant-mass spectrum as well as for the angular distribution,

$$
\mathrm{d}\Gamma(\Upsilon(5S) \to \Upsilon(2S)\pi^+\pi^-)/\mathrm{d}\cos\theta,
$$

can be reconciled with the data, if the $Z_b$'s are included into the analysis as intermediate states.

---

$^4$ Here and in what follows proper combinations with a given $C$-parity are understood, for example, $B\bar{B}^*$ is a shorthand notation for $\frac{1}{\sqrt{2}}(B\bar{B}^* + \bar{B}B^*)$.
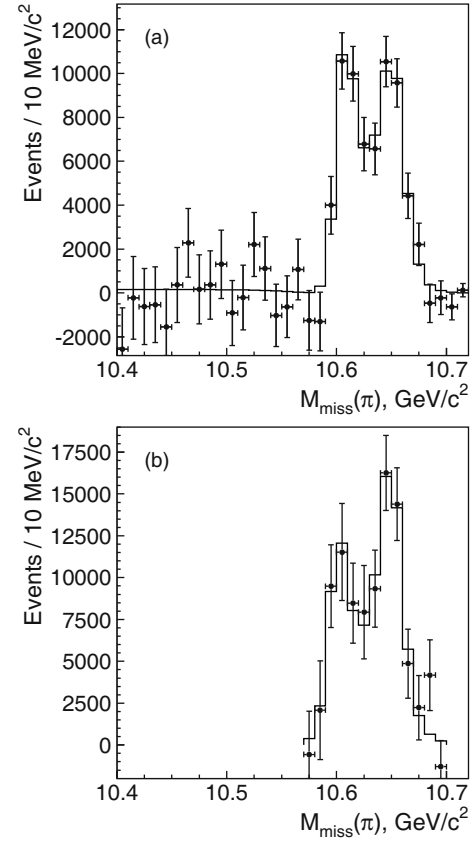


**Fig. 8.** The (a) $\Upsilon(5S) \to h_b(1P)\pi^+\pi^-$ and (b) $\Upsilon(5S) \to h_b(2P)\pi^+\pi^-$ yields as a function of the pion missing mass (adapted from [18]).
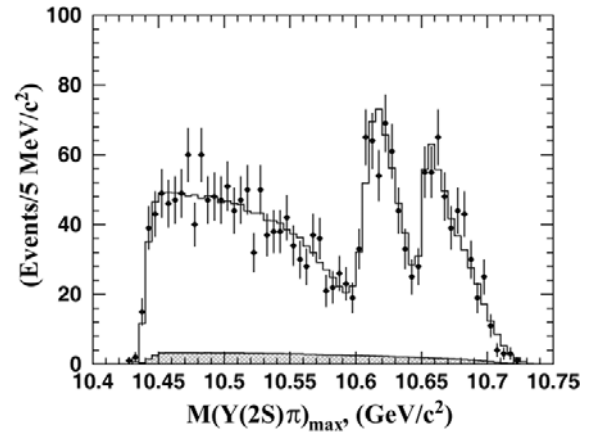


**Fig. 9.** One-dimensional projection of the data for the decay $\Upsilon(5S) \to \Upsilon(2S)\pi^+\pi^-$ (adapted from [18]).

According to the updated analysis [18] (in line with the original report [17]), the Breit-Wigner masses of the $Z_b$ and $Z_b'$ states lie just above the $B\bar{B}^*$ and $B^*\bar{B}^*$ thresholds, respectively. Theoretical work [39], taking into account the coupling to the intermediate $B\bar{B}^*$ and $B^*\bar{B}^*$ states, shows that $Z_b$ masses slightly below the corresponding thresholds are also consistent with the data in the $h_b(1P)\pi^+\pi^-$ and $h_b(2P)\pi^+\pi^-$ (see the comparison in fig. 10). In any
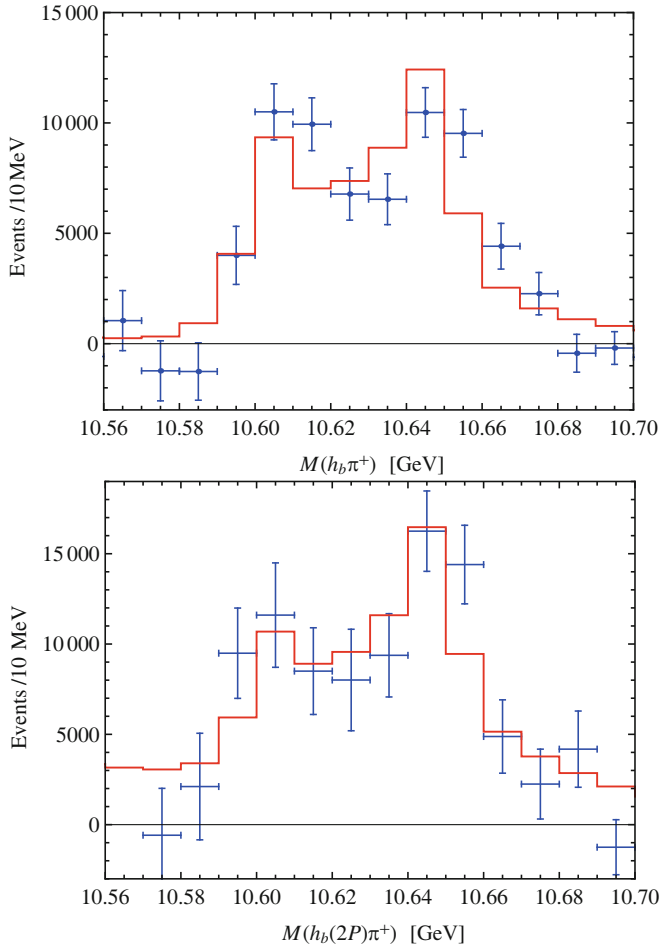
**Fig. 10.** Comparison of the invariant-mass spectra of $h_b\pi^+$ and $h_b(2P)\pi^+$ calculated in [39] with the measured missing-mass spectra $MM(\pi)$.



**Fig. 11.** The fundamental building block (kernel to be iterated) of the coupled-channel scheme in eq. (8) [42].

**Table 1.** Branching fractions in per cent for the $Z_b$ states [46].

| Mode | $Z_b(10610)^+$ | $Z_b(10650)^+$ |
|---|---|---|
| $\Upsilon(1S)\pi^+$ | $0.32 \pm 0.09$ | $0.24 \pm 0.07$ |
| $\Upsilon(2S)\pi^+$ | $4.38 \pm 1.21$ | $2.40 \pm 0.63$ |
| $\Upsilon(3S)\pi^+$ | $2.15 \pm 0.56$ | $1.64 \pm 0.40$ |
| $h_b(1P)\pi^+$ | $2.81 \pm 1.10$ | $7.43 \pm 2.70$ |
| $h_b(2P)\pi^+$ | $4.34 \pm 2.07$ | $14.8 \pm 6.2$ |
| $B^+\bar{B}^{*0} + c.c.$ | $86.0 \pm 3.6$ | – |
| $B^{*+}\bar{B}^{*0}$ | – | $73.4 \pm 7.0$ |

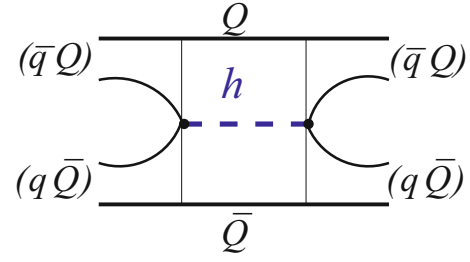case, given the proximity of the $Z_b$ states to these two-body $S$-wave thresholds, the latter are expected to have a strong impact on the properties of the $Z_b$'s. In particular, the analysis in [39] is based on the assumption that the $Z_b$'s are shallow bound states. An alternative interpretation of their resonant nature suggested in [40] is based on the observation that the Belle data are consistent with the $Z_b$'s as threshold cusps.

A coupled-channel approach to hadron spectroscopy near the open-bottom thresholds was developed in [41]. In particular, meson exchange potentials between $B^{(*)}$ mesons at threshold were derived and the corresponding Schrödinger equations were solved numerically. As a result, the masses of the twin $Z_b$ resonances were reproduced and a number of other possible bound and/or resonant states in other channels were predicted. Decay modes suggested for the experimental searches of the predicted states can be found in [41].

An alternative explanation for the $Z_b$ states is proposed in [42], which employs a coupled-channel scheme (see fig. 11),

$$(q\bar{Q})(Q\bar{q}) \leftrightarrow (Q\bar{Q})h, \qquad (8)$$

with $Q$ and $q$ standing for the heavy ($b$) and light quark, respectively, and with $h$ denoting a light hadron (pion). Such an approach is based on the concept of the QCD string breaking with pion emission (further details can be found in [45]). In particular, for the $\Upsilon(nS)$ dipion decays this scheme implies multiple iterations of the basic building block $B^{(*)}\bar{B}^{(*)} \leftrightarrow \Upsilon(nS)\pi$. The calculated production rates for the transitions $\Upsilon(5S) \to \Upsilon(nS)\pi^+\pi^-$ ($n = 1, 2, 3$) reveal peaks at the $B\bar{B}^*$ and $B^*\bar{B}^*$ thresholds. This computation does not assume any direct interaction between $B^{(*)}$ mesons, so that the $Z_b$ singularities appear solely due to the interchannel coupling (8). Similar calculations of the $\Upsilon(5S)$ dipion transitions into $h_b(nP)\pi^+\pi^-$ final state constitute a challenge being addressed by theorists with these tools.

Additional measurements of the Belle Collaboration on the $Z_b$'s have very recently been reported [46]. Two additional observation modes of the $Z_b$ states seem to have been found. They are $\Upsilon(5S) \to \bar{B}B^*\pi(B\bar{B}^*\pi)$ and $\Upsilon(5S) \to B^*\bar{B}^*\pi$, and the $Z_b(10610)$ and $Z_b(10650)$ were found in the missing-mass spectra of the pion in the $\bar{B}B^*\pi$ ($B\bar{B}^*\pi$) and $B^*\bar{B}^*\pi$ final states, respectively. Assuming that the $\Upsilon(1S, 2S, 3S)\pi$, $h_b(1P, 2P)\pi$ and $B^{(*)}\bar{B}^* + c.c.$ modes saturate the decays of the $Z_b$ states, the reported branching fractions are listed in table 1. Furthermore, evidence for the neutral partners of the charged $Z_b$'s was observed in the $\Upsilon(5S) \to \Upsilon(2S)\pi^0\pi^0$. Clearly, the models proposed for the $Z_b$ states have to be confronted with the new data.

Additional insight on the nature of near-threshold resonances can be obtained from an unbiased analysis of the data in the region below threshold. Indeed, in the appropriate mode, the bound state should reveal itself as a peak below the corresponding open-bottom thresholds

in the line shape. In particular, data on radiative decays of the $Z_b$ states could potentially confirm or rule out their bound-state interpretation. To this end, high-statistics and high-resolution data in the region below the nominal $B^{(*)}\bar{B}^*$ thresholds is needed to study the radiative transitions $Z_b(10610) \to B\bar{B}\gamma$, $Z_b(10650) \to B\bar{B}\gamma$, and $Z_b(10650) \to B^*\bar{B}\gamma$. As mentioned above, bound states would reveal themselves as below-threshold peaks which, given the expected high-statistics data from a future $B$-factory, can potentially be observed.

To summarise, a data sample expected to be collected by a high-luminosity $B$-factory with the known production reaction should be sufficient to perform a high-statistics analysis, to exclude alternative interpretations, and to fix the parameters of the $Z_b$ states to a high accuracy, in particular their position relative to the corresponding $B^{(*)}\bar{B}^*$ thresholds. A sophisticated line shape form, respecting unitarity and accounting for threshold vicinity, should be used for the data analysis. The production of the $Z_b$'s can be further investigated at the $\Upsilon(6S)$ energy, and the additional information would be helpful in identifying their nature.

## 2.3 $W_{bJ}$ states

The idea put forward in [35] that the $Z_b$ and $Z_b'$ states can be explained as molecule-type structures residing at the corresponding $B^{(*)}\bar{B}^*$ thresholds was extended further in [35,47,48] and a possible existence of a few sibling states, denoted as $W_{bJ}^{(\prime)}$ with $J = 0, 1, 2$ and defined by four orthogonal combinations,

$$1^-(2^+)\ W_{b2} : \left. 1_{b\bar{b}} \otimes 1_{q\bar{q}} \right|_{J=2},$$

$$1^-(1^+)\ W_{b1} : \left. 1_{b\bar{b}} \otimes 1_{q\bar{q}} \right|_{J=1},$$

$$1^-(0^+)\ W_{b0}' : \left. \frac{\sqrt{3}}{2} 0_{b\bar{b}} \otimes 0_{q\bar{q}} + \frac{1}{2} 1_{b\bar{b}} \otimes 1_{q\bar{q}} \right|_{J=0},$$

$$1^-(0^+)\ W_{b0} : \left. \frac{\sqrt{3}}{2} 1_{b\bar{b}} \otimes 1_{q\bar{q}} \right|_{J=0} - \frac{1}{2} 0_{b\bar{b}} \otimes 0_{q\bar{q}}, \quad (9)$$

was predicted and their properties were outlined. The mesonic components of the $W_{b2}$, $W_{b1}$, $W_{b0}'$ and $W_{b0}$ are the $B^*\bar{B}^*$, $(B\bar{B}^* + B^*\bar{B})/\sqrt{2}$, $B^*\bar{B}^*$ and $B\bar{B}$, respectively.

It has to be noticed that, since the binding mechanisms responsible for the formation of the $Z_b$'s are still obscure, only model-dependent conclusions can be made concerning the existence or non-existence of the $W_b$'s. In particular, if the binding mechanism operates in the $S_{q\bar{q}} = 1$ channel (or in both $S_{q\bar{q}} = 0$ and $S_{q\bar{q}} = 1$ channels), then all four $W_b$'s are expected to exist. However if this mechanism operates only in the $S_{q\bar{q}} = 0$ channel, then only two sibling states ($W_{b0}$ and $W_{b0}'$) are predicted. In what follows it is assumed that all four $W_b$'s exist and the corresponding predictions found in the literature are quoted and discussed.

To proceed, it is convenient to adopt the classification scheme suggested in [47] exploiting the heaviness of the $b$ quark, that implies that its spin is decoupled from the remaining degrees of freedom, so that a convenient basis can be built in terms of the states $H \otimes SLB$, where $H$ stands for the heavy pair spin ($S_H = 0, 1$), while $SLB$ denotes all remaining degrees of freedom, like angular momentum, light-quark spins, etc. In particular, this basis matches naturally the decompositions (7) and (9) above, if $SLB$ is associated with the light-quark total spin $S_{q\bar{q}}$ [47]. Since the $H$ degree of freedom plays the role of a spectator in all decay processes, it is sufficient to just pick up the term with the appropriate $H \otimes SLB$ structure in the final state in order to extract the corresponding decay amplitude. Although a detailed microscopic theory is needed to predict each individual decay width, relative coefficients between different decay widths can be evaluated solely using these simple symmetry-based considerations. Such predictions are [47]

$$\Gamma[Z_b] = \Gamma[Z_b'], \quad (10)$$

$$\Gamma[W_{b1}] = \Gamma[W_{b2}] = \frac{3}{2}\Gamma[W_{b0}] - \frac{1}{2}\Gamma[W_{b0}'] \quad (11)$$

and [48]

$$\Gamma[Z_b] = \Gamma[Z_b'] = \frac{1}{2}\left(\Gamma[W_{b0}] + \Gamma[W_{b0}']\right). \quad (12)$$

Relation (10) can be verified with the help of the Belle measurement of the $Z_b$'s widths (eqs. (5) and (6) above) and indeed it is approximately fulfilled.

Further predictions for specific decay channels follow from the structure of the wave functions (7) and (9), as explained above. In particular [47],

$$\Gamma[W_{b0} \to \Upsilon\rho] : \Gamma[W_{b0}' \to \Upsilon\rho] : \Gamma[W_{b1} \to \Upsilon\rho]$$
$$: \Gamma[W_{b2} \to \Upsilon\rho] = \frac{3}{4} : \frac{1}{4} : 1 : 1, \quad (13)$$

or, similarly [48]

$$\Gamma[W_{b0} \to \eta_b l] : \Gamma[W_{b0}' \to \eta_b l] : \Gamma[Z_b \to \Upsilon l]$$
$$: \Gamma[Z_b' \to \Upsilon l] = \frac{1}{2} : \frac{3}{2} : 1 : 1, \quad (14)$$

$$\Gamma[W_{b0} \to \chi_{b1} l] : \Gamma[W_{b0}' \to \chi_{b1} l] : \Gamma[Z_b \to h_b l]$$
$$: \Gamma[Z_b' \to h_b l] = \frac{3}{2} : \frac{1}{2} : 1 : 1, \quad (15)$$

where $l$ denotes a suitable configuration of light hadrons. It should be noted however that relations (13)–(15) rely only on the structure of the amplitudes in the strict heavy-quark symmetry limit. These predictions acquire corrections due to the hyperfine splitting, conveniently parameterised in terms of the difference $M_{Z_b'} - M_{Z_b}$ [47,48] as well as due to the difference in kinematic phase space. With these effects taken into account and within an effective Lagrangian technique with binding contact interaction, the

following predictions were obtained in [48]:

$$\Gamma[W_{b0} \to \pi\eta_b(3S)] : \Gamma[W'_{b0} \to \pi\eta_b(3S)] :$$
$$\Gamma[Z_b \to \pi\Upsilon(3S)] : \Gamma[Z'_b \to \pi\Upsilon(3S)]$$
$$= 0.26 : 2.0 : 0.62 : 1 \quad (\lambda_\Upsilon \to 0),$$
$$= 0.12 : 2.1 : 0.41 : 1 \quad (|\lambda_\Upsilon| \to \infty),$$

where $\lambda_\Upsilon$ is a certain combination of various coupling constants appearing in the effective Lagrangian (see [48]).

## 2.4 X$_b$ and Y$_b$ states

As argued in [35,49], isovector $Z_b$ and $W_{bJ}$ states may possess isoscalar C-odd and C-even partners, also residing at the $B^{(*)}\bar{B}^{(*)}$ thresholds. There is no general consensus in the literature concerning the naming scheme for such states, so, for the sake of definiteness, we refer to the C-even partners as $X_b$'s (in analogy with the C-even $X(3872)$ charmonium state) while we use the notation $Y_b$'s for C-odd states[5]. It should be noticed that, while C-even states can be structured as $B\bar{B}$, $\frac{1}{\sqrt{2}}(B\bar{B}^* + \bar{B}B^*)$ or $B^*\bar{B}^*$, only two structures, $\frac{1}{\sqrt{2}}(B\bar{B}^* - \bar{B}B^*)$ and $B^*\bar{B}^*$, are allowed for the C-odd states. As a result $X_b$'s can have the $J^{PC}$ quantum numbers $0^{++}$, $1^{++}$, and $2^{++}$ while only the $1^{+-}$ option is available for $Y_b$'s. Then, similarly to the famous $X(3872)$ charmonium, $X_b$'s and $Y_b$'s can mix with the conventional $^3P_J$ and $^1P_1$ bottomonium states, respectively, that makes possible to produce such states through their quarkonium (compact) components in high-energy collisions. Then $Y_b$'s states, should they exist and be produced in an experiment, could be sought for, for example, using the decays $Y_b \to \Upsilon(nS)\eta^{(\prime)}$, $Y_b \to \Upsilon(nS)\pi\pi$, or $Y_b \to \Upsilon(nS)K\bar{K}$ [35]. Similarly, $X_b$'s might be seen in the mode $X_b \to \Upsilon(1S)\omega$ [35].

Finally, it is argued in [49] that, while the C-odd isoscalar $Y_b$ states are not directly accessible in the $\Upsilon(5S)$ decays (neither in radiative decays nor in hadronic transitions), studies of the ratio $R_c/R_n$ (of its deviation from unity) of the yields for pairs of charged and neutral $B^{(*)}$ mesons in the decays $\Upsilon(5S) \to \pi^0 B^{(*)}\bar{B}^{(*)}$ may give an insight on the interaction of $B^{(*)}$ mesons in the isoscalar channel. In particular, in presence of a near-threshold isoscalar resonance, the isospin breaking Coulomb effect provides a specific behaviour of this ratio which can potentially be studied by the future $B$-factories.

The search for the $W_b, X_b, Y_b$ partners of the putative exotic $Z_b$ states could also be conducted with any data taken at the $\Upsilon(6S)$ resonance, which would facilitate additional phase space for the search. Spin splittings for states involving light quarks (as the $Z_b$'s have due to their electric charge) are of order one or two hundred MeV, as, for example, the $h_1(1170)$–$f_2(1270)$ splitting in the light meson spectrum. Since the $Z_b$ candidates have masses in the 10605–10650 MeV range, the $\Upsilon(5S)$ at 10876 MeV may be too light as a starting point to reconstruct decay chains

---

[5] The authors of [35] follow this scheme, however the notation $X_b$ is used in [49] for C-odd states too.

containing the $W_b$, $X_b$, and $Y_b$ partners. The $\Upsilon(6S)$ state at 11020 MeV, on the other hand, offers the safety of the additional phase space, that will allow setting of more extensive exclusion limits and offer larger discovery potential.

## 2.5 Radiative decays of $\Upsilon$(5S)

A recent BaBar analysis using $(111 \pm 1) \times 10^6$ $\Upsilon(3S)$ and $(89 \pm 1) \times 10^6$ $\Upsilon(2S)$ events [50] allowed one to observe $\Upsilon(3S) \to \gamma\chi_{b0,2}(1P)$ decay and to make precise measurements of the branching fractions for the $\chi_{b1,2}(1P, 2P) \to \gamma\Upsilon(1S)$ and $\chi_{b1,2}(2P) \to \gamma\Upsilon(2S)$ decays. A search for the $\eta_b(1S)$ and $\eta_b(2S)$ states was performed in the decays $\Upsilon(nS) \to \gamma\eta_b(n'S)$ ($n = 2, 3; n' < n$), however the significance of the result obtained was insufficient to draw conclusions regarding the $\eta_b(nS)$ masses, so that more data are needed.

Data expected with future high-luminosity $B$-factories at the $\Upsilon(5S)$ energy will allow precise studies of the radiative decays $\Upsilon(5S) \to \gamma\eta_b(nS)$ and $\Upsilon(5S) \to \gamma\chi_{b0,1,2}(mP)$ which meets challenges provided by the lattice and model theoretical calculations of various $\eta_b$ and $\chi_b$ meson properties (hyperfine splittings with the $\Upsilon(nS)$ states, total widths, various decay branching fractions, and so on).

Meanwhile the Belle Collaboration announced [51] a successful identification (with the significance of $15\sigma$) of the $\eta_b(1S)$ state in the decay chain $\Upsilon(5S) \to Z_b^+\pi^- \to h_b(1P)\pi^+\pi^- \to \gamma\eta_b\pi^+\pi^-$. The measured hyperfine splitting $M(\Upsilon(1S)) - M(\eta_b(1S))$ appeared to be lower than the world average by about 10 MeV, and this improves the agreement of the data with lattice simulations as well as with pNRQCD theoretical predictions. Remarkable progress was achieved by using the large sample of data for the $h_b(1P)$ state collected at the energy of the $\Upsilon(5S)$ resonance. Related searches for $h_b(2P)$ radiative decays are expected soon.

Generally, a missing mass method for $\gamma$, $\pi^0$, and $\eta$ can be applied with the higher statistics expected at the future $B$-factories, however it will require longer chains with additional requirements, like the decay $\eta_b(nS) \to \Upsilon(mS)\gamma$ with $m < n$.

The conjecture of the existence of $W_{bJ}$'s, negative $G$-parity isovector partners of the $Z_b$'s, opens extra opportunities for the future $B$-factories in what the $\Upsilon(5S)$ radiative decays are concerned. Indeed, because of the $G$-parity, a natural way these $W_{bJ}$ states could be produced from the $\Upsilon(5S)$ are radiative decays of the latter, as shown in fig. 12 (adapted from [47]). Although such radiative decays are suppressed by the fine structure constant $\alpha = 1/137$ as compared, for example, to $\Upsilon(5S) \to Z_b^{(\prime)}\pi$ decays, the statistics expected at the future $B$-factories should be sufficient to observe such decays.

$\Upsilon(5S)$ is produced in the $e^+e^-$ annihilation, so that there are two possible $b\bar{b}$ configurations, $S$- and $D$-wave, that when combined with spin yield the production quantum numbers $1^{--}$. In the non-relativistic approximation for $b$ quarks only the $S$-wave contribution is retained.
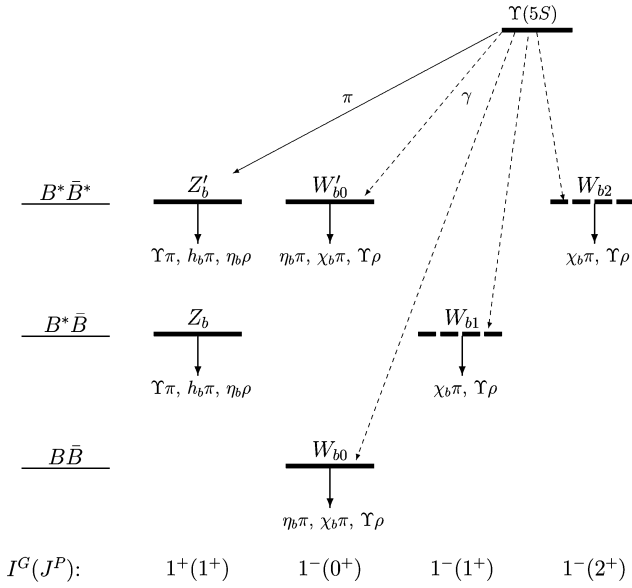
**Fig. 12.** Schematic representation for various closed-flavour decay chains of the $\Upsilon(5S)$ decays, including radiative transitions with conjectured, new $W_{bJ}$ states created at intermediate stages (adapted from [47]).

Then only the $^3S_1$ component of the $\Upsilon(5S)$ wave function is considered which has the following decomposition in terms of the $H \otimes SLB$ states: $1^-_H \otimes 0^+_{SLB}$, where the $H$ component comes from the total $b\bar{b}$ spin while the $SLB$ component accounts for the angular momentum [47]. Such identification leads, in particular, to the following prediction [47]:

$$\Gamma(\Upsilon(5S) \to W_{b0}\gamma) : \Gamma(\Upsilon(5S) \to W'_{b0}\gamma) :$$
$$\Gamma(\Upsilon(5S) \to W_{b1}\gamma) : \Gamma(\Upsilon(5S) \to W_{b2}\gamma)$$
$$= \frac{3}{4}\omega_0^3 : \frac{1}{4}\omega_2^3 : 3\omega_1^3 : 5\omega_2^3 \approx 8.5 : 1 : 21 : 20, \qquad (16)$$

where $\omega_0 \approx 305\,\mathrm{MeV}$, $\omega_1 \approx 260\,\mathrm{MeV}$, and $\omega_2 \approx 215\,\mathrm{MeV}$ are the photon energies in the corresponding transitions.

In fig. 12 various cascade reactions for the $\Upsilon(5S)$ decays are shown graphically, specifically its radiative transitions with $W_{bJ}$'s created in the intermediate state. Measurements of such decay chains may become one of the most promising tasks for the future $B$-factories.

## 2.6 Extraction of the light-quark mass ratio

It was noticed recently that the light-quark mass ratio $\frac{m_u}{m_d}$ can be extracted to high accuracy from data for bottomonium decays [52]. Specifically, the decays $\Upsilon(4S) \to h_b(1P)\pi^0$ and $\Upsilon(4S) \to h_b(1P)\eta$ are useful because the bottom meson loops are highly suppressed in these reactions [52]. Similarly, decays of $\Upsilon(5S)$ into $h_b(nP)\pi^0(\eta)$ should provide the same information on the $\frac{m_u}{m_d}$ ratio. Having a high-statistics measurement from a $B$-factory would be useful to estimate the systematics.

To be specific, a combination of the light-quark mass ratios [53,54],

$$r_{\mathrm{DW}} \equiv \frac{m_d - m_u}{m_d + m_u} \frac{m_s + \hat{m}}{m_s - \hat{m}}$$
$$= \frac{4}{3\sqrt{3}} r_{G\tilde{G}} \frac{F_\pi}{F_\eta} \frac{F_K^2 M_K^2 - F_\pi^2 M_\pi^2}{F_\pi^2 M_\pi^2}(1 - \delta_{\mathrm{GMO}})$$
$$\times \left[1 + \frac{4L_{14}}{F_\pi^2}(M_\eta^2 - M_\pi^2)\right]$$
$$= 10.59\,(1 + 132.1\,L_{14})\,r_{G\tilde{G}}, \qquad (17)$$

can be related to the ratio of the branching fractions of the decays of the $\Upsilon(5S) \to h_b(nP)\pi^0(\eta)$. Here, $\hat{m}$ is the averaged mass of the up and down quarks, $F_{\pi,K,\eta}$ are the meson decay constants, $\delta_{\mathrm{GMO}} = -0.06$ denotes deviation from the Gell-Mann-Okubo relation among the light meson masses, $L_{14} = (2.3 \pm 1.1) \times 10^{-3}$ is a low-energy constant in the $\mathcal{O}(p^4)$ chiral Lagrangian [53,54], and $r_{G\tilde{G}}$ is a ratio of the gluonic matrix elements $\langle 0|G\tilde{G}|\pi^0\rangle/\langle 0|G\tilde{G}|\eta\rangle$. The relation reads

$$\frac{\Gamma(\Upsilon(5S) \to h_b(nP)\pi^0)}{\Gamma(\Upsilon(5S) \to h_b(nP)\eta)} = r_{G\tilde{G}}^2 \left|\frac{\boldsymbol{q}_\pi}{\boldsymbol{q}_\eta}\right|. \qquad (18)$$

Then with additional information on the strange quark mass from elsewhere, one is able to extract the ratio $\frac{m_u}{m_d}$. However, as will be argued below, only the decays into the $h_b(2P)$ can be used.

The light-quark mass ratio has to be extracted from isospin breaking and $SU(3)$ breaking processes. Heavy quarkonium transitions with an emission of a pion or $\eta$ are of potential use. However, coupled-channel effects from the intermediate heavy meson loops are often important in the transitions between two heavy quarkonia. In that case, a large amount of the isospin breaking is provided by the mass difference between the charged and neutral heavy mesons, and hence such decays (for example, $\psi' \to J/\psi\pi^0(\eta)$ [32]) are not suitable for the extraction of the $\frac{m_u}{m_d}$ ratio. Therefore, one must be sure that the heavy meson loops give a small contribution to the transition amplitudes so they do not invalidate the quark mass ratio extraction. An advantage of bottomonium transitions is that the $B$ meson mass difference $M_{B^0} - M_{B^+}$ is about 10 times smaller than the quark mass difference $m_d - m_u$, so that the bottom meson loops in the isospin breaking bottomonium transitions are indeed suppressed. Furthermore, because $|M_{b\bar{b}} - 2M_B| \ll M_B$, the bottomed-meson velocity $v$ is small and the system is non-relativistic. Therefore a power counting approach in the framework of non-relativistic effective field theory can be used to analyse $\eta$-emitting transitions [33]. It turns out that the bottom meson loops are always important in transitions between two $S$-wave as well as two $P$-wave bottomonia. However, for the single-$\eta$ transition amplitude between a $P$-wave and a $S$-wave bottomonium, the effect of the loops can be estimated as [33,55]

$$\frac{\mathcal{A}^{\mathrm{loop}}}{\mathcal{A}^{\mathrm{tree}}} \sim \frac{\boldsymbol{q}^2}{v^3 M_B^2}, \qquad (19)$$

**Table 2.** PDG values for the branching fractions (BF) of two-body $\Upsilon(5S)$ decays.

| Mode | $B\bar{B}$ | $B^*\bar{B} + $c.c. | $B^*\bar{B}^*$ | $B_s\bar{B}_s$ | $B_s^*\bar{B}_s + $c.c. | $B_s^*\bar{B}_s^*$ |
|---|---|---|---|---|---|---|
| BF, % | $5.5 \pm 1.0$ | $13.7 \pm 1.6$ | $38.1 \pm 3.4$ | $0.5 \pm 0.5$ | $1.5 \pm 0.7$ | $17.9 \pm 2.8$ |

where $\boldsymbol{q}$ is the three-momentum of the $\eta$ in the rest frame of the decaying bottomonium and $M_B$ is the mass of the intermediate bottom meson. Decay of $\Upsilon(5S)$ provides enough phase space to produce both $h_b(1P)\eta$ and $h_b(2P)\eta$ final state. For the decay $\Upsilon(5S) \to h_b(1P)\eta$

$$|\boldsymbol{q}| = 771 \,\mathrm{MeV}, \quad v \approx 0.5, \quad \text{so that} \quad \frac{\boldsymbol{q}^2}{v^3 M_B^2} \sim 0.7,$$

which implies that loops are not negligible and this mode cannot be used for the quark mass ratio extraction. In the meantime, for the decay mode $\Upsilon(5S) \to h_b(2P)\eta$,

$$|\boldsymbol{q}| = 274 \,\mathrm{MeV}, \quad v \approx 0.3, \quad \text{so that} \quad \frac{\boldsymbol{q}^2}{v^3 M_B^2} \sim 0.2.$$

This ensures considerable suppression of the bottom meson loops (uncertainty arising due to the loop contributions is of the order of 20%). Hence, this mode, together with its counter-part mode $\Upsilon(5S) \to h_b(2P)\pi^0$, is suitable for the quark mass ratio extraction.

## 3 Open-flavour analysis and $\Upsilon(5S)$ internal structure

Important information can be also obtained from various $\Upsilon(5S)$ decays to open-flavour final states, where the $b$-$\bar{b}$ pair separate into different final-state mesons. Among them, decays to two-body final states are of a special interest because these decays can be precisely measured experimentally and reliably calculated theoretically. Good measurements are also important as benchmarks for the high-energy nuclear physics experimental programme where open-flavour decays of heavy quarkonia are used as probe of high-density nuclear matter [56]. The branching fractions (BF) for all six available open-flavour decays $\Upsilon(5S) \to B_x\bar{B}_x$ have been measured [57] and the results are shown in table 2.

### 3.1 Problems with light-quark $SU(3)$ flavour symmetry

Open-flavour hadron decays entailing light quarks are often fruitfully analysed with the help of $SU(3)$ flavour symmetry. The assumption underpinning effective theory analysis is that hadrons are pointlike particles at small energy scales, and $SU(3)$ symmetry relates the couplings of the parent state to the various decay channels.

With the $\Upsilon(5S)$ being a $SU(3)$ flavour singlet (as natural for a $b\bar{b}$ state), $SU(3)$ is badly broken by the branching fractions shown in table 2 (as will be demonstrated below in this section).

Had $SU(3)$ flavour symmetry been exact, the couplings of the $\Upsilon(5S)$ to the $B^0\bar{B}^0$, $B^+B^-$ and $B_s^0\bar{B}_s^0$ would all have been the same. In practice one would expect some deviations in the branching fractions due to phase space differences (the strange quark being somewhat heavier). But these will turn out to be larger than expected, see eq. (21) below.

Furthermore, a naive application of heavy-quark spin symmetry would entail that the couplings to the vector bottom mesons would also be the same. Therefore, all six open-flavour decays should be related to each other, with their decay amplitudes proportional to the same coupling constant. Thus, all difference in the branching fractions should be related to the decay kinematics.

In detailed calculations, because the $\Upsilon(5S)$ width is large when compared to the difference between its mass and the thresholds of certain channels, such as $B_s\bar{B}_s^*$ and $B_s^*\bar{B}_s^*$, one should take into account the finite-width effect when calculating its decay widths into the open-bottom mesons. A typical decay formula reads

$$\Gamma = \frac{1}{W} \int_{w_{\min}^2}^{(M_\Upsilon+2\Gamma_\Upsilon)^2} \mathrm{d}s \, \frac{(2\pi)^4}{2\sqrt{s}} \int \mathrm{d}\Phi_2 |\mathcal{A}|^2 \frac{1}{\pi}$$
$$\times \mathrm{Im}\left(\frac{-1}{s - M_\Upsilon^2 + iM_\Upsilon\Gamma_\Upsilon}\right), \tag{20}$$

where $M_\Upsilon$ and $\Gamma_\Upsilon$ are the mass and width of the $\Upsilon(5S)$, respectively, see eq. (1), $w_{\min} = \max(M_\Upsilon - 2\Gamma_\Upsilon, m_1 + m_2)$ with $m_1$ and $m_2$ the masses of the bottom mesons in the final state, $\int \mathrm{d}\Phi_2$ denotes the two-body phase space, and $\mathcal{A}$ is the decay amplitude. The factor $1/W$ is included in order to normalise the spectral function of the $\Upsilon(5S)$, and it can be calculated as

$$W = \int_{w_{\min}^2}^{(M_\Upsilon+2\Gamma_\Upsilon)^2} \mathrm{d}s \, \frac{1}{\pi} \mathrm{Im}\left(\frac{-1}{s - M_\Upsilon^2 + iM_\Upsilon\Gamma_\Upsilon}\right).$$

Thus, in the $SU(3)$ limit, the ratios of the branching fractions of all the open-bottom decay modes can be obtained by eliminating the coupling implicit in $|\mathcal{A}|^2$, assuming that it is the same for every channel,

$$B\bar{B} : [B^*\bar{B} + c.c.] : B^*\bar{B}^* : B_s\bar{B}_s : [B_s^*\bar{B}_s + c.c.] : B_s^*\bar{B}_s^*$$
$$= 1 : 3.21 : 12.95 : 0.16 : 0.36 : 0.78. \tag{21}$$

However, slightly different ratios result from the measurements shown in table 2,

$$B\bar{B} : [B^*\bar{B} + c.c.] : B^*\bar{B}^* : B_s\bar{B}_s : [B_s^*\bar{B}_s + c.c.] : B_s^*\bar{B}_s^*$$
$$= 1 : (2.49 \pm 0.54) : (6.93 \pm 1.40) : (0.09 \pm 0.09)$$
$$: (0.27 \pm 0.14) : (3.25 \pm 0.78). \tag{22}$$
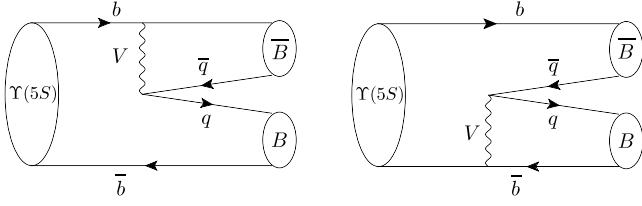
**Fig. 13.** Diagrams used to calculate the open-flavour decays of $\Upsilon(5S)$ in [59].

The largest deviations from the $SU(3)$ limit occur in the vector channels $B^*\bar{B}^*$ and $B_s^*\bar{B}_s^*$, and they occur in opposite directions. So, the experimental value,

$$B_s^*\bar{B}_s^* : B^*\bar{B}^* = 0.47 \pm 0.08,$$

is one order of magnitude larger than the $SU(3)$ value of 0.06. This means that the coupling of the $\Upsilon(5S)$ to the strange vector channel $B_s^*\bar{B}_s^*$ is stronger than that of the non-strange vector channel $B^*\bar{B}^*$ by a factor of 2. Normally, $SU(3)$ breaking does not exceed 30%.

Such a huge $SU(3)$ breaking must have a dynamical origin. One possibility is that the $\Upsilon(5S)$ cannot be taken as a pure light flavour singlet. The possibility of an isospin-1 state is ruled out by the decays of $\Upsilon(5S)$ into the bottom-strange mesons. It would be more subtle if the structure around the $\Upsilon(5S)$ contained a sizable tetraquark component [11,12,58], see sect. 4.2, with the light-quark part of the wave function being purely an isoscalar $(a(|u\bar{u} + d\bar{d}\rangle) + b|s\bar{s}\rangle)$.

Another possibility that we address in the next subsection, is that the internal structure of the parent bottomonium state enhances the kinematic differences between light quarks *at the coupling level*.

## 3.2 Internal $b\bar{b}$ structure

We now turn to the structure of the parent state. In [59], the branching fractions in table 2 were calculated in a model with the Hamiltonian (:: stand for normal ordering)

$$H_I = \frac{1}{2}\sum_{k=1}^{8}\int \mathrm{d}^3x\mathrm{d}^3y : \left[\psi^\dagger(\boldsymbol{x})\frac{\lambda_k}{2}\psi(\boldsymbol{x})\right]V(\boldsymbol{x}-\boldsymbol{y})$$

$$\times \left[\psi^\dagger(\boldsymbol{y})\frac{\lambda_k}{2}\psi(\boldsymbol{y})\right] :, \tag{23}$$

given by the quark colour densities interacting via the Cornell potential,

$$V(r) = -\frac{\kappa}{r} + \frac{r}{a^2}. \tag{24}$$

The corresponding diagrams are shown in fig. 13. It was noticed then that the decay amplitude $A_{5S}(P)$ is an oscillating function of $P$ (the centre-of-mass momentum of the $B$ mesons in the final state), so that its value changes dramatically from one decay channel to another (see fig. 14),
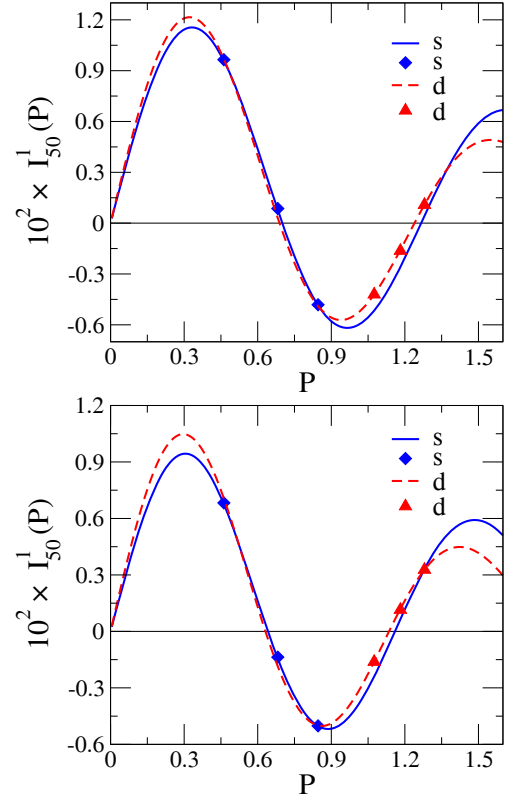


**Fig. 14.** The position of the final momentum $P$ of the $B$ meson for each mode in the $\Upsilon(5S)$ rest frame for two different sets of model parameters. The decay amplitude $A_{5S}$ is related to the quantity $I_{50}^1$ through a simple numerical factor (see [59] for the details).

that may provide an explanation of the data presented in table 2.

In [60,61] the formalisation of these statements, to reduce model dependence, exploited the analogy between open-flavour $\Upsilon(5S)$ decays and the Franck-Condon factorisation in molecular physics (therefore the term "heavy quark fluorescence" used). The central idea of the approach is a so-called "velocity superselection rule" encompassed, for example, in the leading order of such effective theories for QCD with heavy quarks as potential Non-Relativistic QCD (pNRQCD) and Heavy Quark Effective Theory (HQET). This rule states that the heavy quark does not change its velocity upon emitting or interacting with the light degrees of freedom, such as light quarks, gluons, pions, and so on, with a momentum of $\mathcal{O}(\Lambda_{\mathrm{QCD}})$. This entails that the momentum distribution of the heavy mesons in open-flavour decays should be proportional to the momentum distribution of the heavy quarks inside the parent hadrons, thus giving a window to their internal structure [60,61].

In mathematical terms, the momentum $k$ and velocity $v$ of the final $B_x$ meson are related to those of the $b$ quark as

$$k = k_b + \mathcal{O}(\Lambda_{QCD}), \quad v = v_b + \mathcal{O}(\Lambda_{QCD}/M),$$
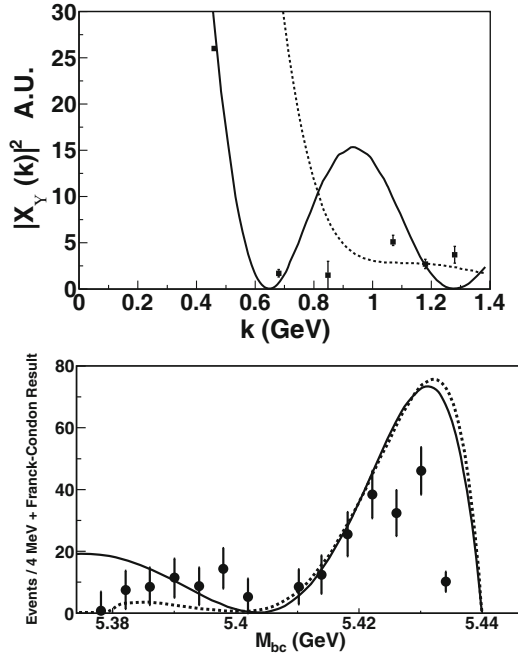
**Fig. 15.** Open-flavour decays of the $\Upsilon(5S)$ resonance as a probe of the $b$-quark wave function squared (adapted from [61]). Upper panel (two-body decays): data points are, from right to left, for the channels $B\bar{B}$, $B\bar{B}^* + B^*\bar{B}$, $B^*\bar{B}^*$, $B_s\bar{B}_s$, $B_s\bar{B}_s^* + B_s^*\bar{B}_s$, $B_s^*\bar{B}_s^*$; the solid curve is for the Coulomb-gauge model wave function of the $\Upsilon(5S)$. Lower panel (three-body decays): data points are for $B^{(*)}\bar{B}^{(*)}\pi$ decays. Here $M_{bc} \equiv \sqrt{(M_\Upsilon/2)^2 - k^2}$. The experimental data, taken from [62] and [63], are divided by the decay phase space factor, by the spin factor, and by an isospin factor 2 for the non-strange decays. The remainder is proportional to the wave function squared. The dashed curves include a $^3P_0$-vertex model computation.

so that one has a leading-order factorisation theorem

$$\mathcal{A}_{\Upsilon \to B_x \bar{B}_x}(k) = \int q^2 \mathrm{d}q \, \psi_\Upsilon(q) \langle b\bar{b}(q) | H_{\mathrm{int}} | B_x \bar{B}_x(k) \rangle$$
$$\simeq F(k)\psi_\Upsilon(k), \tag{25}$$

in analogy to the above-mentioned Franck-Condon factorisation in molecular physics.

   Therefore, to extract information about the wave function squared $|\psi_\Upsilon(k)|^2$ in bottomonium one needs to measure the $B$ meson momentum distributions in various open-flavour decays. In particular, in the two-body $B_s^*\bar{B}_s^*$ channel, the $B_s^*$ meson possesses a relatively small momentum $k$ and therefore this channel probes the central maximum of the wave function, as depicted in fig. 15 (top).

   For the three-body channels (fig. 15, bottom), the zero seen in the solid line is a Sturm-Liouville zero (a generic prediction of quantum mechanics that requires orthogonality between all $nS$ bottomonia, and thus requires the wave functions of excited states to vanish). Since this zero is present in $\psi_\Upsilon(k)$, it should manifest itself in all open-flavour decays and, in particular, one should expect a dip in the three-body $BB^*\pi$ channel [60]. With the

high-statistics available at the future $B$-factories, it should be possible to confirm or to refute the dip in the $B$ meson momentum plot.

# 4 Non-$b\bar{b}$ vector states at $\Upsilon(5S)$ energy

In this section we consider the possibility of existence for an alternative (non-conventional $b\bar{b}$) vector state residing in the region of mass near 10860 MeV. We resort to the notation $Y_b$ for this vector state to distinguish it from the $\Upsilon(5S)$ bottomonium discussed above. Notice that the vector $Y_b$ from this section should not be confused with the hadronic molecules discussed in sect. 2.4.

## 4.1 b$\bar{\mathrm{b}}$g vector hybrid

Since the very beginning of the QCD era, excitations of the glue attracted a lot of attention of both theorists and experimentalists. Indeed, due to the non-Abelian nature of the interaction mediated by gluons, the latter can either play a role of extra constituents of hadrons (hybrid mesons) or form a new type of compounds —glueballs made entirely of two, three, or more gluons. Although there is no general consensus on whether hybrids and glueballs have indeed been observed experimentally, a number of promising candidates exist in various parts of the spectrum of hadrons. In particular, lattice simulations are known to predict the lowest bottomonium hybrid ($b\bar{b}g$) to lie around 10900(100) MeV [64], that is exactly in the region accessible with $B$-factories. With the high-statistics, high-resolution, and low-background data from future $B$-factories in perspective, especially in view of the proximity of the expected mass of the vector bottomonium hybrid to the mass of the $\Upsilon(5S)$ state, it is important to outline specific features inherent to bottomonium hybrids which would allow one to distinguish them from conventional mesons.

### 4.1.1 The radial wave function and the momentum distribution in open-flavour decays of the vector hybrid

A number of theoretical approaches to hybrids has been discussed in the literature, such as lattice simulations [64–70], bag model [71,72], flux tube model [73], Coulomb-gauge QCD model [74–76], potential quark model [77], constituent gluon model [78–80], QCD string model [81–88].

   For the sake of clarity, respective cartoons for the ordinary meson and for the single-gluon hybrid in the framework of the QCD string model are shown in fig. 16. Notice that excitation of the gluonic degree of freedom brings a large contribution to the mass of the state, so that the lowest (not excited radially) hybrid meson has a mass comparable with that of the highly radially excited ordinary meson. Therefore, one can distinguish the radially excited $\Upsilon(5S)$ quarkonium state and the hybrid $Y_b$ by the different patterns of their radial quark-antiquark wave functions
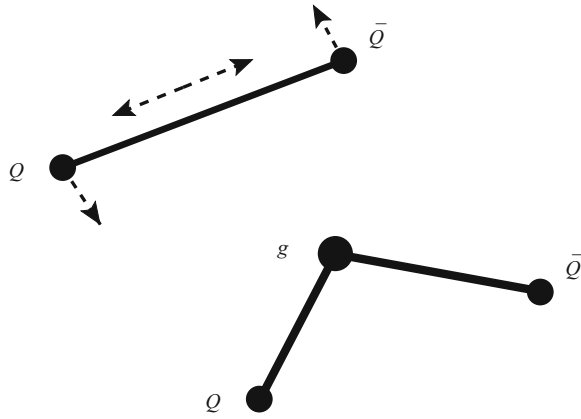
**Fig. 16.** Three possible types of excitations of the QCD string with quarks at the ends: rotation and radial motion correspond to conventional mesons (first plot) while the string vibrations, described in terms of constituent gluons attached to the string, correspond to hybrids (second plot).

(4-node wave function *versus* nodeless wave function). As argued in [60], the shape of the $b\bar{b}$ wave function translates into the $B\bar{B}$ momentum distribution for the three-body final $B\bar{B}\pi$ state, so that it is possible to make a conclusion concerning the source of the $B\bar{B}$ pair: smooth distribution would identify the source as the hybrid while the distribution with residual (after smearing due to the quark recoil in $B$ mesons) structures would indicate a conventional quarkonium as the corresponding source. In fig. 17 this idea is exemplified by the charmonium $\psi(4400)$ resonance, for which the existing Belle and BaBar open-flavour $D_{(s)}^{(*)}\bar{D}_{(s)}^{(*)}$ decays data are used. A similar analysis could be carried out for bottomonium resonances decaying to the open-flavour $B_{(s)}^{(*)}\bar{B}_{(s)}^{(*)}$ channels.

### 4.1.2 Sibling states

One of the most prominent features of hybrids is the fact that exotic quantum numbers, such as $1^{-+}$ forbidden for a conventional quarkonium, are accessible for hybrids. Indeed, once a hybrid possesses a gluon as an extra degree of freedom as compared to the conventional quark-antiquark state, then this new degree of freedom contributes to the $C$- and $P$-parities of the system. In particular, for the constituent gluon or for the QCD string model, the quantum numbers of a one-gluon hybrid are

$$P = (-1)^{l_{q\bar{q}}+j}, \quad C = (-1)^{l_{q\bar{q}}+s_{q\bar{q}}+1}, \quad (26)$$

for the "magnetic" gluon ($l_g = j$), and

$$P = (-1)^{l_{q\bar{q}}+j+1}, \quad C = (-1)^{l_{q\bar{q}}+s_{q\bar{q}}+1}, \quad (27)$$

for the "electric" gluon ($l_g = j \pm 1$), where $l_g$ is the relative angular momentum between the $q\bar{q}$ pair and the gluon, $j$ is the total angular momentum of the gluon, $l_{q\bar{q}}$ is the orbital momentum in the quark-antiquark subsystem, and $s_{q\bar{q}}$ is the spin of the quark-antiquark pair.
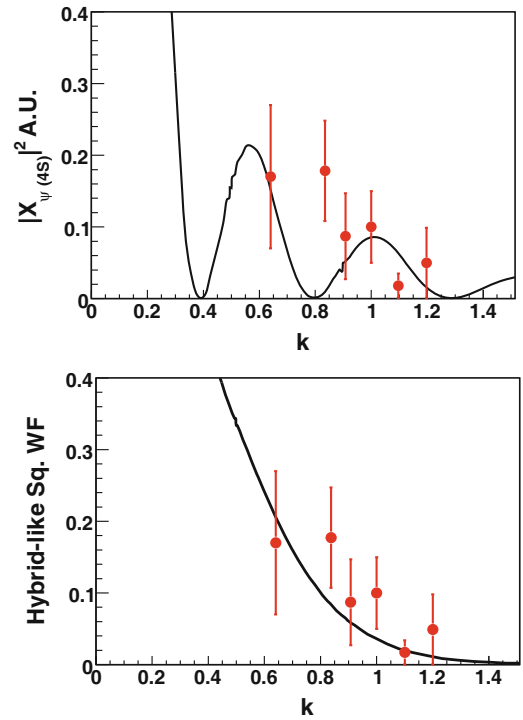


**Fig. 17.** Pure $c\bar{c}(4S)$ (first) *versus* charmonium hybrid (second) hypothesis (solid lines) for the $\psi(4400)$ decaying to open-flavour. The solid lines are typical model-wave functions, and the coarse data are our adaption of various BaBar and Belle measurements of the 2-body branching fractions for $D\bar{D} \dots D_s^* \bar{D}_s^*$ dividing by known spin and isospin factors.

The vector quantum numbers of highest interest for $e^+e^-$ colliders can be achieved therefore both for the electric gluon,

$$s_{q\bar{q}} = 1, \quad l_{q\bar{q}} = 1, \quad l_g = 0, 2, \quad j = 1, \quad (28)$$

as well as for the magnetic gluon,

$$s_{q\bar{q}} = 0, \quad l_{q\bar{q}} = 0, \quad l_g = 1, \quad j = 1. \quad (29)$$

However, hybrids with an electric gluon couple too strongly to two $S$-wave final-state mesons and, as estimated in [80], do not exist as resonances. On the contrary, for hybrids with a magnetic gluon, a selection rule is established (see, for example, [79,80,84,89–91]) which forbids its $B_{(s)}^{(*)}\bar{B}_{(s)}^{(*)}$ decay modes, so that the lowest possible open-beauty modes are the ones with one $S$-wave and one $P$-wave $B$ meson (see below).

The lowest states with magnetic gluons have $l_{q\bar{q}} = 0$. Then the $1^{--}$ hybrid is a spin-singlet state with respect to the quark spin,

$$|1^{--}\rangle_m = \Phi(r,\rho)S_0(q\bar{q})\sum_{\nu_1\nu_2}C_{1\nu_1 1\nu_2}^{1m}\rho Y_{1\nu_1}(\hat{\rho})S_{1\nu_2}(g),$$

$$(30)$$

and there are three other hybrid states, with $J^{-+}$, $J = 0, 1, 2$, lying in the vicinity of the vector hybrid. These are
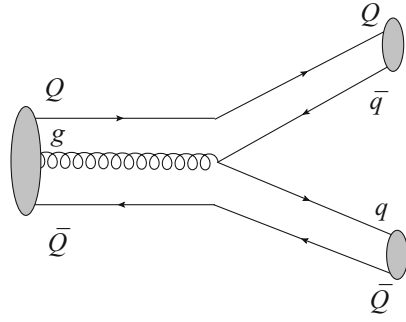
**Fig. 18.** Graphical representation for a $Q\bar{Q}g$ hybrid open-flavour decay.

spin triplets,

$$|J^{-+}\rangle_m = \Phi(r,\rho) \sum_{\mu_1\mu_2} C^{Jm}_{1\mu_1 1\mu_2} S_{1\mu_1}(q\bar{q})$$

$$\times \sum_{\nu_1\nu_2} C^{1\mu_2}_{1\nu_1 1\nu_2} \rho Y_{1\nu_1}(\hat{\rho}) S_{1\nu_2}(g), \qquad (31)$$

where $S_{1\nu}(g)$ is the spin wave function of the gluon, $S_0(q\bar{q})$ and $S_{1\nu}(q\bar{q})$ are the singlet and triplet spin wave functions of the $q\bar{q}$ pair, $\Phi(r,\rho)$ is the radial wave function in momentum space. The four states (30) and (31) are expected to be degenerate in the heavy-quark limit, with the degeneracy removed by spin-dependent quark-gluon interactions.

The prediction for hybrids is therefore that, together with the vector hybrid, three more sibling hybrid states with the quantum numbers $(0,1,2)^{-+}$ should exist in the same region of mass.

### 4.1.3 Open-flavour decay pattern

Schematic representation of the single-gluon hybrid open-flavour decay is given in fig. 18. With the form of the wave functions (30) and (31) in hand, it is straightforward to calculate the corresponding $Y_b \to \bar{B}(1S)B(1S)$ and $Y_b \to \bar{B}(1S)B(1P)$ recoupling coefficients [86][6]. In table 3 such coefficients are listed for the vector hybrid. Similar coefficients for the siblings can be found in [86]. As was mentioned above, all coefficients $Y_b \to B(1S)\bar{B}(1S)$ vanish.

The vector hybrid decay modes into $\bar{B}B_J$ with $J = 0, 1, 2$, followed by the decays $B_J \to B^{(*)}\pi$ (currently known modes are $B_1 \to B^{*+}\pi^-$, $B_2 \to B^{*+}\pi^-$, and $B_2 \to B^+\pi^-$), populate the final states $\bar{B}^*B\pi$ and $\bar{B}B\pi$. Notice that decays into $\bar{B}^{(*)}B_J$ are not allowed because of the mass threshold.

---

[6] Notice that here and in what follows, where it applies, charge conjugated components of the $Y_b$ wave function are omitted for simplicity and an obvious shorthand notation is used, for example, $\bar{B}(1S)B(1P) \equiv \frac{1}{\sqrt{2}}(\bar{B}(1S)B(1P) + B(1S)\bar{B}(1P))$.

To summarise, the vector hybrid $Y_b$ is expected

– to contribute to the three-body $B\bar{B}^{(*)}\pi$ final states;
– to possess three hybrid siblings with the mass splittings about 20–40 MeV between each other and with the vector $Y_b$ and with quantum numbers $J^{-+}$ $J = 0, 1, 2$, including the exotic one $1^{-+}$;
– to have a different $\bar{B}B$ momentum distributions in the final $\bar{B}B\pi$ state than conventional $b\bar{b}$ quarkonium.

### 4.1.4 A scan between $\Upsilon(4S)$ and $\Upsilon(5S)$

The proliferation of vector charmonium or charmonium-like states above threshold, that includes at least $\psi(3770)$, $\psi(4040)$, $\psi(4160)$, $Y(4260)$, $\psi(4400)$, $Y(4360)$, $Y(4660)$, makes clear that not all can be pure charmonium states, as the quark model cannot support such a multiplicity of mesons.

The $b\bar{b}$ system, with better spaced narrow resonances, is a system where more clarity can be achieved, especially concerning the existence or non-existence of similar non-$b\bar{b}$ excitations. The BaBar Collaboration [1] has conducted a scan between 10.5 and 11.2 GeV with 300 energy steps and about 25 inverse picobarn per step, with additional data around the $\Upsilon(6S)$ resonance.

Only the putative $\Upsilon(5S)$ and $\Upsilon(6S)$ states at 10860 MeV and 11020 MeV were revealed by this scan. Thus, the room for hybrid mesons shrinks to two options. Either the narrower vector hybrid is part of one of these two resonances, or if its mass is elsewhere in the interval of interest (as predicted by theory), its $e^+e^-$ coupling is very small and higher beam intensity is needed to produce it. This is not totally unexpected in view of the difficulty of exciting the flux tube by an electromagnetic current. Thus, a rescan of this energy range with increased luminosity would be welcome (the mass resolution reached by BaBar is sufficient for this application and does not need to be increased).

Additionally, BaBar observed a cross-section dip due to interference at the $B_s\bar{B}_s$ threshold, but no structure at around 11100–11200 MeV, which is the energy where the pair of quarks $bs$ and antiquarks $\bar{b}\bar{s}$ can first be produced in an $S$-wave. This could be rechecked, and it would be interesting to examine whether any sign of the positive-parity $B_s$ mesons appears in the total $b$ cross-section.

Funally, it would be interesting to examine exclusive channels with closed flavour, such as $\Upsilon^{(\prime)}\pi\pi$ and $\Upsilon^{(\prime)}KK$ in this mass range, because the analogous $Y$ resonances in the charmonium spectrum do not appear as bumps in the total charm cross-section, but rather exhibit themselves in the $\psi^{(\prime)}\pi\pi$ distributions. In particular, some of the $Y$ states may be understood as hadro-charmonia [92], such as the $Y(4660)$ as a $\psi' f_0(980)$ bound state [93]. Such kind of states would be more visible in the closed-flavour than the open-flavour final states. Analogously, there can be hadro-bottomonia which can be searched for in the $\Upsilon^{(\prime)}\pi\pi$ and $\Upsilon^{(\prime)}KK$ distributions using the initial-state radiation (ISR) technique.

**Table 3.** Spin recoupling coefficients for the vector hybrid. Here $B^{(*)}$ is an $S$-wave $B^{(*)}$ meson and $B_J$ is a $P$-wave $B$ meson with the total momentum $J$.

| Channel | $\bar{B}B$ | $\bar{B}B^*$ | $\bar{B}^*B^*$ | $\bar{B}B_0$ | $\bar{B}^*B_0$ | $\bar{B}B_1(^1P_1)$ | $\bar{B}^*B_1(^1P_1)$ | $\bar{B}B_1(^3P_1)$ | $\bar{B}^*B_1(^3P_1)$ | $\bar{B}B_2$ | $\bar{B}^*B_2$ |
|---|---|---|---|---|---|---|---|---|---|---|---|
| Coefficient | 0 | 0 | 0 | 0 | $\frac{1}{\sqrt{6}}$ | 0 | $-\frac{1}{2}$ | $\frac{1}{2}$ | $\frac{1}{2\sqrt{2}}$ | 0 | $-\frac{1}{2}\sqrt{\frac{5}{6}}$ |

## 4.2 Vector tetraquark

Tetraquark models [11,94] result in a prediction of existence of two (light and heavy) states, $Y[b, l/h]$, which are linear superpositions of the $J^{PC} = 1^{--}$ tetraquark states $Y[bu] = [bu][\bar{b}\bar{u}]$ and $Y[bd] = [bd][\bar{b}\bar{d}]$. If the mass difference between these two states, estimated as $M(Y[b, h]) - M(Y[b, l]) = (5.6 \pm 2.8)\,\text{MeV}$ [11,94], is neglected, the corresponding degenerate tetraquark states can be considered as a candidate for the vector $Y_b$.

Presence of the light-quark pair in the wave function of the tetraquark $Y_b$ leads to a number of predictions:

– Enhancement of the dipion transitions $Y_b \to \Upsilon(nS)\pi\pi$ ($n < 5$) as compared to the transitions of the conventional quarkonium state, $\Upsilon(5S) \to \Upsilon(nS)\pi\pi$. Predictions of the model are consistent (both for the distributions in the dipion invariant mass and for the helicity angle) [58] with the Belle data [95].
– Model predictions exist for the $K^+K^-$ and $\eta\pi^0$ invariant-mass distributions for the processes $e^+e^- \to Y_b \to \Upsilon(1S)K^+K^-$, and $e^+e^- \to Y_b \to \Upsilon(1S)\eta\pi^0$, respectively. The model [11] predicts the ratio

$$\frac{\sigma(\Upsilon(1S)K^+K^-)}{\sigma(\Upsilon(1S)K^0\bar{K}^0)} = \frac{1}{4}.$$

– The decay widths $Y_b \to h_b(1P)\eta$ and $Y_b \to h_b(2P)\eta$ are expected to be abnormally large, since the OZI suppression does not apply.

It should be noted that the calculations [11] are based on an extra assumption that the low-lying scalar $0^{++}$ states ($f_0(500)$, $f_0(980)$, $a_0(980)$) are tetraquarks.

## 5 Exploration of higher energies: towards the $\Upsilon(11020)$ state and above

In this chapter we review some physics topics that can be addressed if a future $B$-factory can access energies above the $\Upsilon(5S)$ resonance. It includes studies in the region of the last currently known resonance of the bottomonium system, the $\Upsilon(11020)$, as well as the production of triply charmed baryons (for which very clean theoretical predictions are possible) and generally triple charm, and the $\Lambda_b^0\bar{\Lambda}_b^0$ system (that in addition to precision tests of pNRQCD will allow further studies of flavour and $CP$-violation).

## 5.1 Studies at the $\Upsilon(11020)$

It was argued in sect. 4 that, if hybrid bottomonium is discovered, its exotic $J^{PC}$ quantum numbers can be used as a smoking gun, since both flux-tube and quasi-particle models make very specific predictions for their possible combinations.

However, if these states appear around the $\Upsilon(5S)$, their production with the $1^{--}$ quantum numbers in the initial state requires running at a higher energy, so they can appear as intermediate states in various decay chains. In addition, the vector hybrid can be produced directly in ISR processes, that also requires higher energies, around $11\,\text{GeV}$, to be accessible with a future $B$-factory, so it makes sense to take data at $11020\,\text{MeV}$ for spectroscopy studies. An interesting question is whether the $B_s^{(*)}\bar{B}_s^{(*)}$ branching fractions for this resonance can be a source of bottom-strange mesons competitive with the $\Upsilon(5S)$ state.

In addition, one could think of reconstructing the $\omega$ meson in the reaction $\Upsilon(11020) \to \omega\chi_b'$[7]. This would open the second quadruplet of positive-parity, excited $\chi_b'$ mesons, that have been hinted [96] to be precisely at about a mass of 10230 to 10250 MeV, at the end of phase space for the decay involving an $\omega(780)$. Reconstruction of the $\omega$ would also allow to search for the $\eta_b$ ground and first excited state $\eta_b'$ in a channel different from radiative decays [97].

As for testing the nature of the $\Upsilon(11020)$ state itself, it should be noted that additional four-body open-flavour decay channels are open, and therefore several thresholds allow for a detailed mapping of the wave function squared.

A large number of three- and four-body decay channels would allow searches for Sturm-Liouville nodes in the final-state $B$ meson momentum distributions (see fig. 19). Particularly curious might prove the $B_sB_s\pi\pi$ that has a very little phase space but resides near the central wave function maximum.

Some of the three- and four-body final states will however be populated by intermediate $B\bar{B}_J$ ($J = 0, 1, 2$) resonances that need to be separated from the pure multi-body decays. These quasi two-body decays make the $\Upsilon(11020)$

---

[7] One should identify the $\omega$ in the dilepton or triple pion channel, and then plot its momentum and energy spectra in the initial $\Upsilon$ centre-of-mass frame. The recoiling positive-parity meson would appear as a resonance in this. The phase space being so tight, since $11020 - 780 = 10240\,\text{MeV}$, whether the positive-parity state is detected will depend on its precise mass, that might exceed the experimental window. At least a bound can be set.
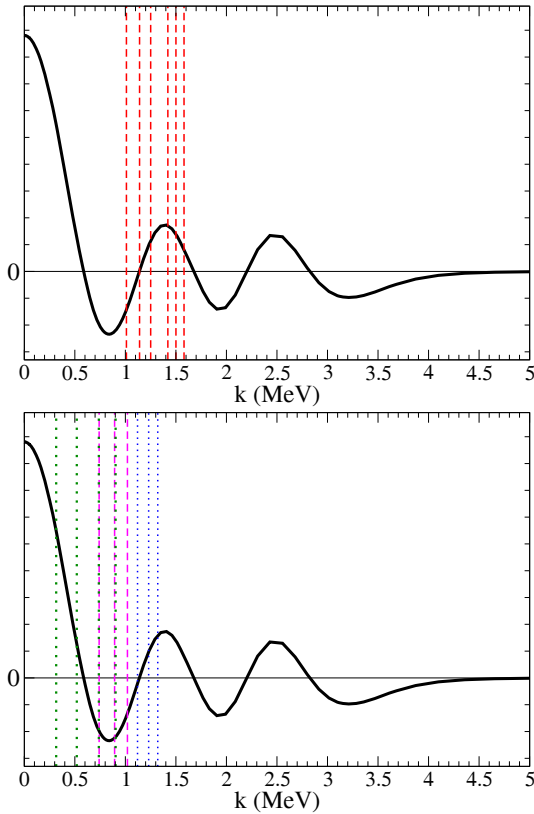
**Fig. 19.** Wave function of the $\Upsilon(6S)$ state (candidate assignment for the $\Upsilon(11020)$ bottomonium). The upper plot shows the position of the six two-body thresholds as function of the final meson (initial quark) momentum. The lower plot shows the three- and four-body thresholds. Interesting is, in spite of its small phase space, the rate of $B_s B_s \pi\pi$ decay, that resides near the central wave function maximum.

a good starting point for studying excitations of the $B$ and $B_s$ mesons.

### 5.2 Search for the Rydberg states of bottomonium

If energies in the range 11.2–11.4 GeV appear to be accessible at a future $B$-factory, further high-lying states in the $b\bar{b}$ spectrum can be searched for. In particular, quark model estimates show that $\Upsilon(7S)$ (see table 4) and $\Upsilon(8S)$ are expected to reside in this region. A relevant worry is of course that these states are predicted broad, with the width of order 150–200 MeV, comparable with their energy separation, so that even using high-resolution data and employing appropriate formulae for overlapping resonances might not allow one to resolve them as separate states. In addition, the value of the wave function at the origin decreases with the radial excitation number, production of higher $S$-wave states being suppressed accordingly. Nevertheless, behaviour of the $R_b$ may still be sensitive to the existence of these highly excited bottomonia.

Another relevant issue is the problem of observation of vector $D$-wave states $\Upsilon(nD)$. Quark models predict a few of them to reside in the region 10.7–11.2 GeV (see

table 4). Although pure $^3D_1$ quark-antiquark states have tiny dileptonic widths, the $S$-$D$–wave mixing provides a mechanism which may increase substantially such a width for the physical meson originated from the pure $^3D_1$ state. It has been argued in [99] that, due to the $S$-$D$ mixing, the dielectron widths of the $\Upsilon(nD)$ bottomonia, with $n = 3, 4, 5$, may be as large as about 100 eV, that is compatible with similar widths of the $\Upsilon((n+1)S)$ states. Together with a high statistics expected to be available at future $B$-factories, this opens a possibility to observe $\Upsilon(nD)$ bottomonia directly in $e^+e^-$ experiments.

### 5.3 $B_J$ mesons

Another possible task for the $\Upsilon(11020)$ studies at the future $B$-factories is the identification of bottomed positive-parity $B_J$ mesons; the present experimental situation is somewhat obscure.

By analogy with other meson families, such as the $D$ mesons, one expects a quadruplet of positive-parity states $(0^+, 1^+, 1^+, 2^+)$, that in the quark model correspond to $P$-wave quark-antiquark mesons. Heavy-quark symmetry suggests to group them in two doublets, $(0^+, 1^+)$ and $(1^+, 2^+)$, with an approximate mass degeneracy within each doublet, as implemented in HQET. The corresponding states are known in the $D$ meson spectrum (upper panel in fig. 20) and a similar pattern is expected naturally for the spectrum of $B$ mesons (lower panel in fig. 20). In table 5 we overview theoretical predictions for the masses of the positive-parity $B_J$ mesons (including predictions of the lattice QCD). In particular, the mass of the $J = 0$ state $B_0$ is estimated to be around 5.7–5.8 GeV or, from the effective chiral/HQET Lagrangian approach (pending publication), to be smaller, about 5700 MeV, with some unitarised chiral Lagrangian studies putting it even lower at 5600 MeV [108–112]. Together with the mass of 5325 MeV for the vector $B^*$ meson, this sets the threshold for the production of this family to be approximately 11 GeV. Therefore, while open-bottom decays of $\Upsilon(5S)$ have all channels $B^{(*)}\bar{B}_J$ kinematically closed, the $S$-wave decay $\Upsilon(11020) \to B^*\bar{B}_0$ may appear to be allowed (it might be no coincidence that there is a resonance at this $S$-wave threshold).

In the meantime, the $B_0$ scalar state has not been observed, so we are forced to rely on theoretical predictions and thus to place it at approximately 5700 MeV and to expect it to be broad (see the lower panel of fig. 20). The expected total width of $B_0$ is of order 100–200 MeV, that may make this state difficult to identify experimentally.

The $2^+$ state, $B_2^*(5747)$, has been observed experimentally, with a small width of $\Gamma = 23(4)$ MeV and decaying to both $B^*\pi$ and $B\pi$ final states with similar branching fractions [57]. Due to its width and the width of the $\Upsilon(10120)$, which is $79\pm16$ MeV [57], this state can in principle also be produced at 11020 MeV energies (the nominal threshold being 11026 MeV).

If the pattern of $D_J$ mesons is taken as a true guide, one expects two $B_1$ mesons, one narrow and one broad,

**Table 4.** Some recent theoretical predictions for the masses (in MeV) of radially excited $S$- and $D$-wave vector states in the bottomonium spectrum.

|  | $4S$ | $3D$ | $5S$ | $4D$ | $6S$ | $5D$ | $7S$ |
|---|---|---|---|---|---|---|---|
| [98] | 10640 | 10700 | 10870 | 10920 | 11075 | 11115 | – |
| [99] | 10645 | 10705 | 10880 | 10928 | 11084 | 11123 | 11262 |
| [100] | 10611 | 10670 | 10831 | 10877 | 11023 | 11060 | 11193 |

**Table 5.** Theoretical predictions for the masses of the $P$-level $B_J$ mesons in MeV (the first six columns). The last two columns contain predictions of lattice QCD and the existing experimental data, respectively. The subscripts 1/2 and 3/2 denote the light-quark total angular momentum, that would be an experimental observable only in the limit of an infinite heavy-quark mass.

|  | [101] | [102] | [103] | [104] | [105] | [106] | [107] | [57] |
|---|---|---|---|---|---|---|---|---|
| $B_0(P_{1/2})$ | 5760 | 5722 | 5738 | 5627 | 5700 | – | 5754 | – |
| $B_1(P_{1/2})$ | 5780 | 5741 | 5757 | 5674 | 5750 | – | 5730 | – |
| $B_1(P_{3/2})$ | 5780 | 5716 | 5719 | – | 5774 | 5755 | 5684 | $5723.5 \pm 2.0$ |
| $B_2^*(P_{3/2})$ | 5800 | 5724 | 5733 | – | 5790 | 5846 | 5770 | $5743 \pm 5$ |
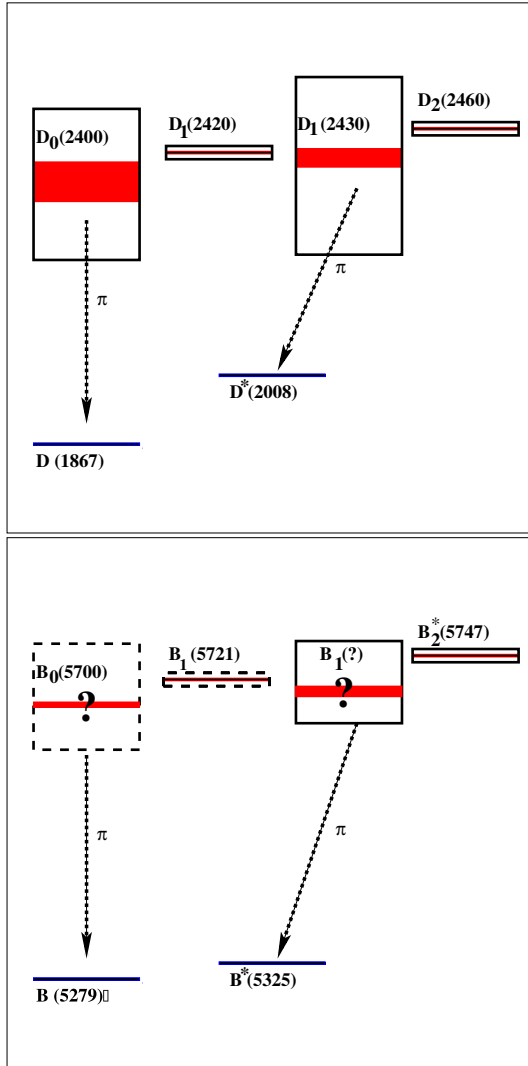


**Fig. 20.** Spectrum of positive-parity $D_J$ and $B_J$ mesons. Expected (but yet unknown) states in the $B$ meson spectrum are tagged with question marks.

producing two nearly degenerate heavy-quark spin symmetry doublets with the $B_0$ and $B_2$ states. One of these $J = 1$ mesons is known as $B_1(5721)$ [57], however its width has not been measured. It most probably is the narrow $P_{3/2}$ doublet partner of the $B_2^*$ meson. Then the other, not yet observed, $B_1$ state should be as light as its $P_{1/2}$ doublet partner $B_0$, and it is expected to be broad. Therefore the decays $\Upsilon(11020) \to B\bar{B}_1$ with both $B_1$'s in the final state should be allowed. The above mentioned missing states are tagged in fig. 20 with question marks.

The conclusion of this discussion is that the positive-parity $B_J$ states can be seen by a future $B$-factory operating at and slightly above the $\Upsilon(11020)$ resonance, with the possibility of discovering two new states, and improving the data quality for the other two.

Production of $B_J$'s is expected to be copious because of the $S$-wave open-bottom threshold appearing near 11020 MeV and, given the fact that $\Upsilon(11020)$ resides exactly at the $B\bar{B}_J$ threshold, it may provide an interesting pattern of threshold phenomena.

The channels $B\bar{B}\pi$, $B\bar{B}\pi\pi$ are promising, and sufficient data may be collected to perform an angular analysis of the $B^{(*)}\pi$ subsystem.

Finally, if data were taken at energies well above the $\Upsilon(11020)$ resonance, a second multiplet of positive-parity $B$ mesons would open. The quark model generically predicts a radial excitation of each member of the $B$ meson family at a cost of about 600 MeV. The unitarised effective Lagrangian method [111,112], that incorporates $SU(3)$ symmetry among light quarks, finds that there are two higher and narrow states in the $0^+$ and $1^+$ sectors. Their masses are larger than the lowest positive-parity states by only 300 MeV. A salient feature is that they strongly couple to channels with hidden strangeness, that is $B_s^{(*)}K$ and $B^{(*)}\eta$. Hence, they are different from the conventional quark model states, whose coupling to the $B^{(*)}\pi(\eta)$ and $B_s^{(*)}K$ should possess an approximate $SU(3)$ flavour symmetry. Interestingly, it is possible that these two higher states are slightly above the $B^{(*)}\eta$ thresholds, and in that
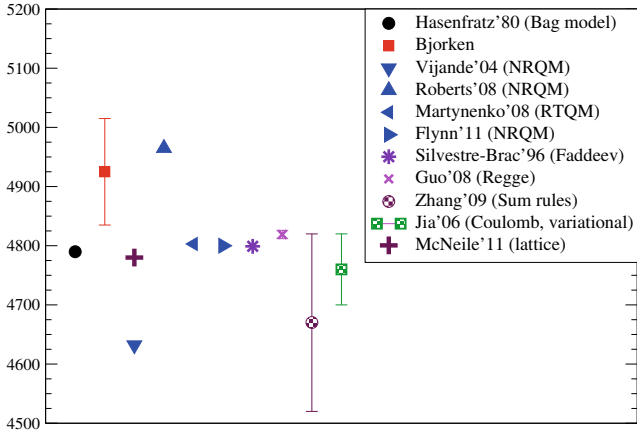
**Fig. 21.** Results of various computations of the ground-state triply charmed baryon.

case, due to the strong coupling, the decays into these modes may even have a width comparable to the $B^{(*)}\pi$. A measurement of the ratio of branching fractions into various channels related through the $SU(3)$ flavour symmetry would be useful to identify the nature of these states.

## 5.4 Triple charm and triply heavy baryons

Double charm and charmonium production have been studied for a long time. In 1987 the WA75 Collaboration started these studies at CERN. In the last decade, the Belle and BaBar Collaborations produced double charm/charmonium [113] reporting, in particular, a large production of the $J/\psi D^{(*)}\bar{D}^{(*)}$ final states. Given an expected high luminosity, triple charm production may become accessible for studies at the future $B$-factories. The minimum energy needed for triple $J/\psi$ production at an electron-positron collider is 9300 MeV, well within the reach of any $B$-factory. The cross-section could potentially be calculated within NRQCD.

The next threshold with increasing energy would be the production of a baryon-antibaryon pair. The relevant ground-state baryon is the $\Omega_{ccc}$, and its spectrum of excitations is of great theoretical importance as this system is expected to be well described in terms of the quark model, so that the given baryon-antibaryon production would be useful to assess applicability of various quark model features to QCD.

The ground-state $\Omega_{ccc}$ has not yet been discovered and its mass is unknown. A spread of predictions obtained in various approaches can be seen in fig. 21. Then, assuming the mass $M(\Omega_{ccc}) \sim 4800$–4900 MeV, the baryon-antibaryon threshold should lay at 9600–9800 MeV. By the time of the planned $B$-factories operation start, further results for the $\Omega_{ccc}$ mass are expected to appear to better pin-down the mass range.

Another interesting threshold for $\Omega_{ccc}$ production is the open-flavour threshold with three recoiling $\bar{D}$ mesons, via the reaction

$$e^+e^- \to \Omega_{ccc}\bar{N}\bar{D}\bar{D}\bar{D}, \qquad (32)$$

that opens up at about $11400 \pm 200$ MeV with the current uncertainty in the $\Omega_{ccc}$ mass. Such processes were studied in [114] with the focus on LEP physics at the $Z$ pole and a prediction for the cross-section of about 0.4 fbarn was obtained. Translated to the properties of a future $B$-factory operating at 11.4 GeV, this estimate would imply cross-sections of order of 3 fbarn, however more theoretical work is clearly needed to make more accurate predictions.

Another very interesting channel is

$$e^+e^- \to \Omega_{ccc}^{++}\bar{\Lambda}_c^-\bar{D}^0D^-. \qquad (33)$$

All particles recoiling in the final state are weakly decaying particles so that the reconstruction could be feasible. The threshold is around 10820–10920 MeV, the same energy range as the $\Upsilon(5S)$, assuming $M(\Omega_{ccc}) \sim 4800$–4900 MeV.

Phenomenology of the $\Omega_{ccc}$ baryon is extensively discussed in [115]. Recently the weak-decay chain

$$\Omega_{ccc} \to \Xi_{ccs}\pi \to \Xi_{css}\pi\pi \to \Omega_{sss}\pi\pi\pi,$$

was stressed in [116] as the most promising avenue, but in view of low statistics one should also consider additional channels with pions replaced by kaons, with the corresponding baryon in the final state being then a nucleon, $\Sigma$ or $\Xi$. Additionally one can employ the recoiling mass technique against the $\bar{D}$ mesons to try to identify the thresholds for the reactions (32), (33).

Finally, an additional physics item can be highlighted, which is the QCD three-body force. QCD is a non-linear theory that features a three-body gluon-gluon coupling not present in electrodynamics. This has been empirically confirmed by the study of four-jet events at colliders. Three-heavy quark baryons offer a window to this three-body force, since the triple gluon coupling also forces a triple-quark potential $V(r_1, r_2, r_3)$ that cannot be decomposed in terms of two-body potentials $V(r_1 - r_2)$ [117]. This has been demonstrated to be relatively small and of order 25–50 MeV for triply charmed baryons, both in model terms [118] and in perturbation theory [119]. Therefore, an electron-positron machine, in particular such as SuperB, could deliver precise data needed to test this QCD feature. Further tests should be developed by theorists by the time, when the planned $B$-factories will start operation.

## 5.5 Pion transition form factor

Perturbative QCD (pQCD) makes specific predictions for exclusive processes, such as hadron form factors at large momentum transfer or exclusive cross-sections at fixed angle and asymptotically large momentum [120]. These predictions encode the Brodsky-Farrar counting rules [121] and entail that relevant couplings in Yang-Mills theory are largely scale-invariant. They are contingent on the hadron distribution amplitudes being finite at the end point when one of the partons carries zero momentum.

The simplest example of the power law behaviour of an exclusive amplitude is the pion form factor. Experimental

data at squared momenta that should already be considered high respect to the hadron $1\,\text{GeV}^2$ scale [122–124] is about a factor of 3 larger than the pQCD prediction.

A much larger squared momentum has been achieved at BaBar and Belle for the transition form factor that controls $\pi_0 \to \gamma^*(Q^2)\gamma$. While the BaBar data are in clear disagreement with the pQCD prediction, the Belle data are less so. In particular, the quantity $Q^2 F(Q^2)$ should be a constant at asymptotically large $Q^2$, as per the QCD counting rules, with the constant also strictly determined by $F(Q^2) \to 2f_\pi/Q^2$ to be $2f_\pi$ at leading order in pQCD. Instead, the BaBar data are better compatible with a growing function rather than with a constant one. This can be accommodated if the end point of the pion distribution amplitude does not vanish because of low-$x$ Regge behaviour [125]. However, the newer Belle data could be compatible with both types of behaviour, although detailed analysis [126] shows that the asymptotic regime has not been reached even at $40\,\text{GeV}^2$ (quite a large scale for hadron structure).

One needs therefore a higher statistics study of the pion transition form factor in the reaction

$$e^+e^- \to e^+e^- \gamma^*\gamma \to e^+e^-\pi^0, \qquad (34)$$

for example, at the energy of the $\Upsilon(4S)$ resonance to reduce the errors of the existing points. However, since, at those high energies, the pion mass is negligible, the maximum $Q^2$ transferred through the virtual photon scales in proportion to the total centre-of-mass energy squared $E_{cm}^2$ of the initial state.

Further data from the future high-luminosity $B$-factories could clarify whether the pQCD counting rules and specific predictions are valid in such exclusive processes or one needs to resort to more sophisticated computations. In particular, increasing the energy from $10.579\,\text{GeV}$ at the $\Upsilon(4S)$ to the $11.020\,\text{GeV}$ at the last $\Upsilon$ resonance entails a moderate 8.5% increase in $Q^2$, so that an additional point in fig. 22 at $50\,\text{GeV}^2$ is conceivable.

### 5.5.1 Testing factorization of $\gamma\gamma^* \to \pi\pi$

Similar tests can be conducted in the quite unexplored reaction

$$e^-e^+ \to \gamma\gamma^*(Q^2)e^-e^+ \to \pi\pi e^-e^+ . \qquad (35)$$

It is important to establish the high $Q^2$ virtuality of one of the photons by means of appropriate cuts on the final-state lepton momenta.

The currently untested pQCD factorization formula for the hadron tensor in this reaction [127],

$$T_{\pi\pi}^{\mu\nu} = -g_T^{\mu\nu} \sum_q \frac{e_q^2}{2} \int_0^1 \frac{2z-1}{z(1-z)} \Phi_q^{\pi\pi}(z, \zeta, E_{\pi\pi}^2)\,\mathrm{d}z, \quad (36)$$

is analogous to the equivalent relation controlling the pion transition form factor in the same approximation,

$$T_\pi^{\mu\nu} = \boldsymbol{\epsilon}^{\mu\nu} \sum_q \frac{e_q^2}{2} \int_0^1 \frac{\mathrm{d}z}{z(1-z)} \phi_q^\pi(z), \qquad (37)$$
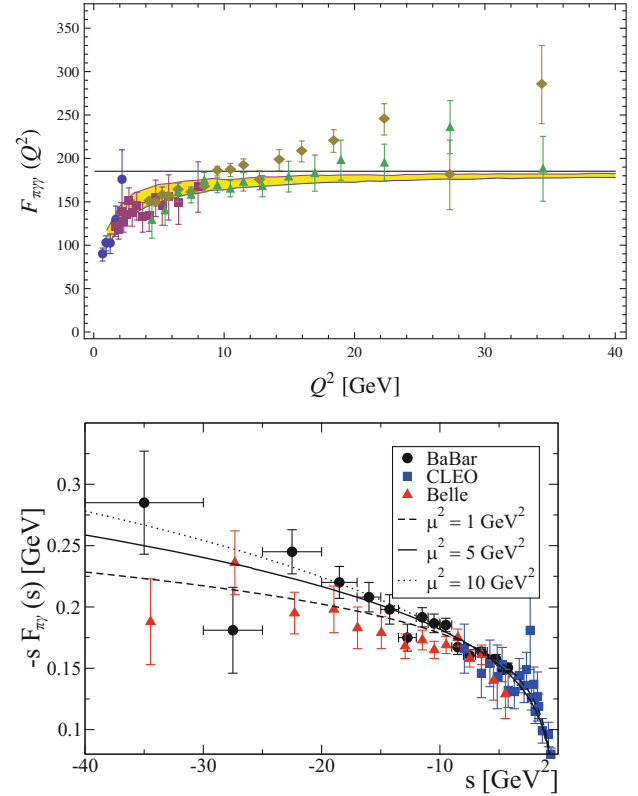


**Fig. 22.** The first plot (courtesy of E. Ruiz Arriola, P. Masjuan, and W. Broniowski) shows a canonical pQCD calculation with two vector mesons to account for the form factor at low-momentum transfer. The second plot (courtesy of A. Szczepaniak) is an additional theory calculation assuming that Regge behaviour dominates the end point of the distribution amplitude.

but substituting the conventional pion distribution amplitude $\phi_q^\pi$ for quark $q$ inside the pion by a Generalized Distribution Amplitude $\Phi_q^{\pi\pi}$ that characterizes the two-pion system (related by crossing to the much discussed Generalized Parton Distributions). Again, in the asymptotic regime where pQCD makes a statement, for $Q^2$ much larger than any other scale, the prediction for the two-pion amplitude is scaling behaviour. At fixed $\zeta$ and $W^2$ the amplitude is predicted to be $Q^2$ independent (in practice one has logarithmic corrections from higher orders in perturbation theory, and subleading negative powers of $Q^2$ from higher-twist corrections, but definitely no positive $Q^2$ power).

Should the test of scaling fail, and the amplitude behave as a positive power of $Q^2$, one should understand the behaviour of $\Phi_q^{\pi\pi}$ near the end points $z = 0, 1$ to appreciate whether it was indeed finite as assumed, and perhaps look for other parametrizations of data. Should scaling be satisfied, then there is a variety of studies that can be performed to learn about hadron structure through these generalized amplitudes from the data [127].

These investigations should help to settle the question of the applicability of pQCD reasoning in exclusive processes, which is one of the outstanding theory predictions requiring testing.

## 5.6 The $\Lambda_b\bar{\Lambda}_b$ threshold

Should the beam energy allow to reach the 11.24 GeV region (in centre of mass), one would encounter the $\Lambda_b\bar{\Lambda}_b$ threshold, where bottomed baryons are first produced. We can see two main reasons to produce a sample of these baryons.

The first is the pursuit of direct $CP$ violation studies in decays. The Particle Data Group [57] collects two measurements of such asymmetries,

$$A_{CP} = \frac{B(\Lambda_b \to f) - B(\bar{\Lambda}_b \to \bar{f})}{B(\Lambda_b \to f) + B(\bar{\Lambda}_b \to \bar{f})} \qquad (38)$$

$A_{CP}(\Lambda_b^0 \to p\pi^-) = 0.03 \pm 0.17 \pm 0.05$ (a very inconclusive measurement) and $A_{CP}(\Lambda_b^0 \to pK^-) = 0.37 \pm 0.17 \pm 0.03$ (that is already a very reasonable hint). The theoretical interest in these and similar asymmetries is that they depend on different QCD matrix elements from those computed for the $B$ meson decay programme, so they will continue overconstraining the CKM picture of quark flavour with different systematics in theory computations.

Note also that the polarisation of the $\Lambda_b$ can be used to test time reversal symmetry $T$ violation [128]. One way to proceed is to reconstruct the decay chain $\Lambda_b \to \Lambda_0 l^+ l^-$ where the two leptons have the invariant mass of a vector meson. Identifying a non-vanishing transverse polarisation of the resulting vector meson or hyperon measures a separation from time-reversal symmetry. Several tests of $P$ and $CP$ violation can also be conducted.

The second major reason is that the dominant decay mode $b \to c$ will typically leave as a remainder a singly charmed baryon [129], and since the $\Lambda_b$ mass at 5619 MeV is so much higher than the $\Lambda_c$ mass at 2290 MeV and above, all charmed baryons are accessible and can be populated, which can assist discovering some additional excited resonances in that spectrum, either by direct reconstruction or by the missing mass technique. Note for example that, while semileptonic decay $\Lambda_b \to \Lambda_c l\bar{\nu}_l$ has a branching fraction of order 6–7%, no single hadronic mode involving $\Lambda_c$ reaches 1%. Thus, many charmed baryons are being produced with a small branching fraction.

Historically, the detection of excited baryons has been pursued in order to assess the "missing resonance problem" (quark models overpredict the number of excited resonances in light baryons). Since baryons with one charm quark tend to be cleaner probes of the excited degrees of freedom, there will be interest in the low-energy hadron physics community to compare any possible new states with the Jefferson-Lab program on light baryons. A theoretical prediction for the $\Lambda_b\bar{\Lambda}_b$ production in $e^+e^-$ collisions can be found in [130].

## 5.7 The $B_c^+B_c^-$ threshold

So far $CP$ violation studies have been carried out extensively with $B\bar{B}$ and $K\bar{K}$ meson pairs, as well as with the $D\bar{D}$ and $B_s\bar{B}_s$ systems. Future studies can break ground in the $B_c\bar{B}_c$ system. The currently measured mass of the
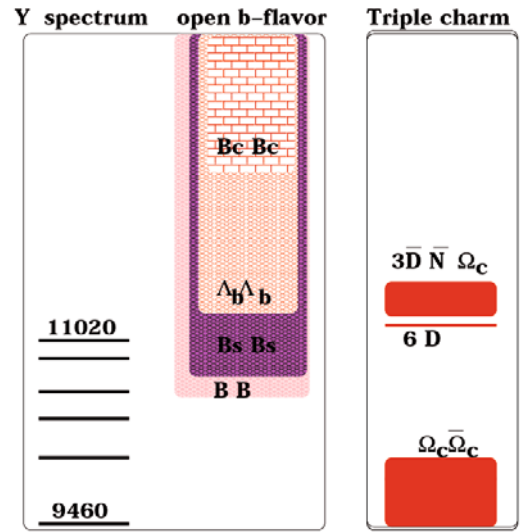


**Fig. 23.** The $\Upsilon$ spectrum and open-$b$ flavour thresholds (left) as well as selected triple charm thresholds (right; $\Omega_c$ here is the $\Omega_{ccc}$ triply charmed baryon).

$B_c$ meson puts the threshold for $B_c\bar{B}_c$ at 12550 MeV, a challenging energy for a $B$-factory designed to operate at the energies up to around 11 GeV. Being realistic, this is perhaps a goal for a machine upgrade after the first five-year running period, but it is worth exploring the implications early on.

Saliently, direct $CP$ violation studies comparing the $B_c$ and $\bar{B}_c$ can help further constrain the Standard Model CKM picture of $CP$ violation [131] (since the $B_c$ mesons are charged, there is no indirect $CP$ violation in this system).

Furthermore, the $B_c$ system is theoretically cleaner than the $B$, $B_s$ systems. Indeed, while one can exploit HQET in the latter two to parametrise theoretical uncertainties into a few quantities, the $B_c$ meson contains two heavy quarks, so that an additional effective theory, Non-Relativistic QCD, is of use, and its potential version pNRQCD allows for perturbative (or semi-perturbative) computations of several quantities of interest, reducing theory uncertainties.

For a taster, in a recent review of the flavour physics of SuperB [132], a stated goal is to measure $V_{bc}$ in the CKM matrix to a precision of 0.5–1%. Such an extraction is theory dominated, and one needs to trust theory to provide the necessary improvements to profit from the future $B$-factories data. This makes the feasibility of the extraction more uncertain. An alternative way to reach this precision, and better, would be to measure the leptonic and semileptonic decays of the $B_c$ meson with reasonable accuracy. Compare with the current situation, at the 2% level, of the $V_{cs}$ measurement, limited by theory computations of the $D_s$ decay constant, $f_{D_s} = 249 \pm 3$ MeV that enters the purely leptonic decays of this meson (and analogously for semileptonic decays). Since the $B_c$ meson is much cleaner theoretically, the requisite theory precisions will be off the shelf for lattice collaborations addressing the issue of $V_{cb}$.

Since the $B_c^+ B_c^-$ system resides well above the open-bottom region, one does not expect prominent resonances to be formed (and none has been found so far). To increase the sample of $B_c$ pairs obtained in a small run, the near-threshold region could be studied in the first place, hoping to find there a cusp or a molecular-type resonance decaying into $B_c^+ B_c^-$. Observing this would, on the other hand, be of tremendous interest for tetraquark studies (that tend to predict bound states of two doubly heavy mesons [133]). Judging by the $B_s$ production off the $\Upsilon(5S)$ resonance, one should expect about 0.01 units of $R$ (the ratio to the $\mu\mu$ production cross-section), or about 5 pbarn, slightly above the $B_c \bar{B}_c$ threshold. With a modest $10 \, \text{fb}^{-1}$ luminosity accumulated during a pilot run, a $B$-factory running at the energy close to the $B_c^+ B_c^-$ mass threshold should produce $50000 \, B_c \bar{B}_c$ pairs. Taking into account that all existing experiments have reconstructed only dozens of these mesons, it could break new ground enormously.

To summarise this section, the physics potential of extending the energy reach with a future $B$-factory running above the $\Upsilon(5S)$ region is depicted in fig. 23. Given the many interesting studies that can be performed, it is worth keeping the possibility open of running the future $B$-factories at a higher energy, with a sensible rooftop at the $B_c^+ B_c^-$ threshold around $12550 \, \text{MeV}$.

# 6 Conclusion

In this paper we outlined hadron physics potential of the planned electron-positron $B$-factories at the $\Upsilon(5S)$ resonance and above. In particular, we stress that the opportunities of a $B$-factory operating at slightly higher energies than the $\Upsilon(4S)$ for a moderate period of time are manifold, involving both fundamental studies of the Standard Model and traditional spectroscopy and hadron structure studies, much increasing the scientific impact of the facility. The basic picture of particle physics between 10.5 and 12.5 GeV has been glimpsed from past lepton accelerators such as LEP, and hadron colliders have produced some of the new particles expected there, but not in sufficient amount nor purity to carry out detailed studies. Some particles expected from theory to be produced in this region remain undiscovered, such as a positive parity $B_1$ meson, or the triply charmed $\Omega_{ccc}$. The search for QCD exotics will receive many new constraints in this region of energy, where hybrid bottomonium resides, according to theory. We look forward to the construction of this exciting machine, and its fruitful operation at high energy.

# References

1. BABAR Collaboration (B. Aubert *et al.*), Phys. Rev. Lett. **102**, 012001 (2009) arXiv:0809.4120 [hep-ex].
2. N. Brambilla, S. Eidelman, B.K. Heltsley, R. Vogt, G.T. Bodwin, E. Eichten, A.D. Frawley, A.B. Meyer *et al.*, Eur. Phys. J. C **71**, 1534 (2011) arXiv:1010.5827 [hep-ph].
3. Belle Collaboration (K.F. Chen *et al.*), Phys. Rev. D **82**, 091106 (2010) arXiv:0810.3829 [hep-ex].
4. C. Meng, K.-T. Chao, Phys. Rev. D **78**, 034022 (2008) arXiv:0805.0143 [hep-ph].
5. Belle Collaboration (K.F. Chen *et al.*), Phys. Rev. Lett. **100**, 112001 (2008) arXiv:0710.2577 [hep-ex].
6. Y.P. Kuang, T.M. Yan, Phys. Rev. D **24**, 2874 (1981).
7. CLEO Collaboration (D. Cronin-Hennessy *et al.*), Phys. Rev. D **76**, 072001 (2007) arXiv:0706.2317 [hep-ex].
8. BABAR Collaboration (B. Aubert *et al.*), Phys. Rev. Lett. **96**, 232001 (2006) arXiv:hep-ex/0604031.
9. Yu.A. Simonov, A.I. Veselov, Phys. Lett. B **671**, 55 (2009) arXiv:0805.4499 [hep-ph].
10. Yu.A. Simonov, A.I. Veselov, Phys. Rev. D **79**, 034024 (2009) arXiv:0804.4635 [hep-ph].
11. A. Ali, C. Hambrock, M.J. Aslam, Phys. Rev. Lett. **104**, 162001 (2010) **107**, 049903(E) (2011) arXiv:0912.5016 [hep-ph].
12. A. Ali, C. Hambrock, S. Mishima, Phys. Rev. Lett. **106**, 092002 (2011) arXiv:1011.4856 [hep-ph].
13. D.-Y. Chen, J. He, X.-Q. Li, X. Liu, Phys. Rev. D **84**, 074006 (2011) arXiv:1105.1672 [hep-ph].
14. D.-Y. Chen, X. Liu, S.-L. Zhu, Phys. Rev. D **84**, 074016 (2011) arXiv:1105.5193 [hep-ph].
15. CLEO Collaboration (F. Butler *et al.*), Phys. Rev. D **49**, 40 (1994).
16. Belle Collaboration (A. Sokolov *et al.*), Phys. Rev. D **75**, 071103 (2007) hep-ex/0611026, BELLE Collaboration (K. Abe *et al.*), hep-ex/0512034.
17. Belle Collaboration (I. Adachi *et al.*), arXiv:1105.4583 [hep-ex].
18. Belle Collaboration (A. Bondar *et al.*), Phys. Rev. Lett. **108**, 122001 (2012) arXiv:1110.2251 [hep-ex].
19. M.B. Voloshin, Y.M. Zaitsev, Sov. Phys. Usp. **30**, 553 (1987) Usp. Fiz. Nauk **152**, 361 (1987).
20. Y.-P. Kuang, Front. Phys. China **1**, 19 (2006) hep-ph/0601044.
21. F.-K. Guo, P.-N. Shen, H.-C. Chiang, R.-G. Ping, Nucl. Phys. A **761**, 269 (2005) hep-ph/0410204.
22. M.B. Voloshin, Phys. Rev. D **74**, 054022 (2006) hep-ph/0606258.
23. M.B. Voloshin, JETP Lett. **37**, 69 (1983) Pisma Zh. Eksp. Teor. Fiz. **37**, 58 (1983).
24. V.V. Anisovich, D.V. Bugg, A.V. Sarantsev, B.S. Zou, Phys. Rev. D **51**, 4619 (1995).
25. F.-K. Guo, P.-N. Shen, H.-C. Chiang, R.-G. Ping, Phys. Lett. B **658**, 27 (2007) hep-ph/0601120.
26. BES Collaboration (M. Ablikim *et al.*), Phys. Lett. B **598**, 149 (2004) hep-ex/0406038.
27. L.S. Brown, R.N. Cahn, Phys. Rev. Lett. **35**, 1 (1975).
28. T. Mannel, R. Urech, Z. Phys. C **73**, 541 (1997) hep-ph/9510406.
29. H.J. Lipkin, S.F. Tuan, Phys. Lett. B **206**, 349 (1988).
30. P. Moxhay, Phys. Rev. D **39**, 3497 (1989).
31. H.-Y. Zhou, Y.-P. Kuang, Phys. Rev. D **44**, 756 (1991).

32. F.-K. Guo, C. Hanhart, U.-G. Meißner, Phys. Rev. Lett. **103**, 082003 (2009) **104**, 109901(E) (2010) arXiv:0907.0521 [hep-ph].

33. F.-K. Guo, C. Hanhart, G. Li, U.-G. Meißner, Q. Zhao, Phys. Rev. D **83**, 2011 (034013) arXiv:1008.3632 [hep-ph].

34. Belle Collaboration (I. Adachi *et al.*), Phys. Rev. Lett. **108**, 032001 (2012) arXiv:1103.3419 [hep-ex].

35. A.E. Bondar, A. Garmash, A.I. Milstein, R. Mizuk, M.B. Voloshin, Phys. Rev. D **84**, 054010 (2011) arXiv:1105.4473 [hep-ph].

36. Y. Yang, J. Ping, C. Deng, H.S. Zong, J. Phys. G **39**, 105001 (2012) arXiv:1105.5935 [hep-ph].

37. Z.F. Sun, J. He, X. Liu, Z.G. Luo, S.L. Zhu, Phys. Rev. D **84**, 054002 (2011) arXiv:1106.2968 [hep-ph].

38. J. Nieves, M.P. Valderrama, Phys. Rev. D **84**, 056015 (2011) arXiv:1106.0600 [hep-ph].

39. M. Cleven, F.-K. Guo, C. Hanhart, U.-G. Meißner, Eur. Phys. J. A **47**, 120 (2011) arXiv:1107.0254 [hep-ph].

40. D.V. Bugg, Europhys. Lett. **96**, 11002 (2011) arXiv:1105.5492 [hep-ph].

41. S. Ohkoda, Y. Yamaguchi, S. Yasui, K. Sudoh, A. Hosaka, Phys. Rev. D **86**, 014004 (2012) arXiv:1111.2921 [hep-ph].

42. I.V. Danilkin, V.D. Orlovsky, Y.A. Simonov, Phys. Rev. D **85**, 034012 (2012) arXiv:1106.1552 [hep-ph].

43. A. Ali, C. Hambrock, W. Wang, Phys. Rev. D **85**, 054011 (2012) arXiv:1110.1333 [hep-ph].

44. M.T. Li, W.L. Wang, Y.B. Dong, Z.Y. Zhang arXiv:1204.3959 [hep-ph].

45. Yu.A. Simonov, A.I. Veselov, Phys. Rev. D **79**, 034024 (2009).

46. Belle Collaboration (I. Adachi *et al.*), arXiv:1209.6450 [hep-ph].

47. M.B. Voloshin, Phys. Rev. D **84**, 031502 (2011) arXiv:1105.5829 [hep-ph].

48. T. Mehen, J.W. Powell, Phys. Rev. D **84**, 114013 (2011) arXiv:1109.3479 [hep-ph].

49. M.B. Voloshin, Phys. Rev. D **86**, 034013 (2012) arXiv:1204.1945 [hep-ph].

50. BABAR Collaboration (J.P. Lees *et al.*), Phys. Rev. D **84**, 072002 (2011) arXiv:1104.5254 [hep-ex].

51. Belle Collaboration (R. Mizuk *et al.*), Phys. Rev. Lett. **109**, 232002 (2012) arXiv:1205.6351 [hep-ex].

52. F.-K. Guo, C. Hanhart, U.-G. Meißner, Phys. Rev. Lett. **105**, 162001 (2010) arXiv:1007.4682 [hep-ph].

53. J.F. Donoghue, D. Wyler, Phys. Rev. D **45**, 892 (1992).

54. J.F. Donoghue, B.R. Holstein, D. Wyler, Phys. Rev. Lett. **69**, 3444 (1992).

55. F.-K. Guo, C. Hanhart, G. Li, U.-G. Meißner, Q. Zhao, Phys. Rev. D **82**, 034025 (2010) arXiv:1002.2712 [hep-ph].

56. B. Friman, S.H. Lee, T. Song, Phys. Lett. B **548**, 153 (2002) nucl-th/0207006.

57. Particle Data Group (J. Beringer *et al.*), Phys. Rev. D **86**, 010001 (2012).

58. A. Ali, C. Hambrock, I. Ahmed, M.J. Aslam, Phys. Lett. B **684**, 28 (2010).

59. D.S. Hwang, H. Son, Eur. Phys. J. C **67**, 111 (2010) arXiv:0812.4402 [hep-ph].

60. I.J. General, S.R. Cotanch, F.J. Llanes-Estrada, Eur. Phys. J. C **51**, 347 (2007) hep-ph/0609115.

61. J.M. Torres-Rincon, F.J. Llanes-Estrada, Phys. Rev. Lett. **105**, 022003 (2010) arXiv:1003.5989 [hep-ph].

62. Belle Collaboration (A. Drutskoy), PoS **EPS-HEP2009**, 056 (2009) arXiv:0909.5223 [hep-ex].

63. A. Drutskoy, arXiv:0905.2959 [hep-ex].

64. K.J. Juge, J. Kuti, C.J. Morningstar, Phys. Rev. Lett. **82**, 4400 (1999).

65. C. Michael, arXiv:hep-ph/0308293.

66. Y. Liu, X.-Q. Luo, Phys. Rev. D **73**, 054510 (2006).

67. X.-Q.Luo, Y. Liu, Phys. Rev. D **74**, 034502 (2006).

68. T. Burch, C. Ehmann, Nucl. Phys. A **797**, 33 (2007).

69. J.J. Dudek, R.G. Edwards, N. Mathur, D.G. Richards, Phys. Rev. D **77**, 034501 (2008).

70. J.J. Dudek, E. Rrapaj, Phys. Rev. D **78**, 094504 (2008).

71. M. Chanowitz, S. Sharpe, Nucl. Phys. B **222**, 211 (1983), **228**, 588(E) (1983).

72. T. Barnes, F.E. Close, F. de Viron, Nucl. Phys. B **224**, 241 (1983).

73. T. Barnes, F.E. Close, E.S. Swanson, Phys. Rev. D **52**, 5242 (1995).

74. S.R. Cotanch, F.J. Llanes-Estrada, Nucl. Phys. A **689**, 481 (2001).

75. I.J. General, S.R. Cotanch, F.J. Llanes-Estrada, Eur. Phys. J. C **51**, 347 (2007) hep-ph/0609115.

76. F.J. Llanes-Estrada, S.R. Cotanch, Phys. Lett. B **504**, 15 (2001) hep-ph/0008337.

77. E. Abreu, P. Bicudo, J. Phys. G **34**, 195207 (2007).

78. D. Horn, J. Mandula, Phys. Rev. D **17**, 898 (1978).

79. A. Le Yaouanc, L. Oliver, O. Pene, J.-C. Raynal, S. Ono, Z. Phys. C **28**, 309 (1985).

80. F. Iddir, S. Safir, O. Pene, Phys. Lett. B **433**, 125 (1998).

81. Yu.A. Simonov, Nucl. Phys. B Proc. Suppl. **23**, 283 (1991).

82. Yu.S. Kalashnikova, Yu.B. Yufryakov, Phys. Lett. B **359**, 175 (1995).

83. Yu.A. Simonov, Phys. At. Nucl. **68**, 1294 (2005).

84. Yu.S. Kalashnikova, Z. Phys. C **62**, 323 (1994).

85. Yu.S. Kalashnikova, D.S. Kuzmenko, Phys. At. Nucl. **66**, 955 (2003).

86. Yu.S. Kalashnikova, A.V. Nefediev, Phys. Rev. D **77**, 054025 (2008) arXiv:0801.2036 [hep-ph].

87. F. Buisseret, C. Semay, Phys. Rev. D **74**, 114018 (2006).

88. F. Buisseret, V. Mathieu, C. Semay, B. Silvestre-Brac, Eur. Phys. J. A **32**, 123 (2007).

89. E. Kou, O. Pene, Phys. Lett. B **631**, 164 (2005).

90. N. Isgur, R. Kokoski, J. Paton, Phys. Rev. Lett. **54**, 869 (1985).

91. F.E. Close, P.R. Page, Nucl. Phys. B **443**, 233 (1995).

92. S. Dubynskiy, M.B. Voloshin, Phys. Lett. B **666**, 344 (2008) arXiv:0803.2224 [hep-ph].

93. F.-K. Guo, C. Hanhart, U.-G. Meißner, Phys. Lett. B **665**, 26 (2008) arXiv:0803.1392 [hep-ph].

94. L. Maiani, F. Piccinini, A.D. Polosa, V. Riquer, Phys. Rev. D **71**, 014028 (2005).

95. Belle Collaboration (K.F. Chen *et al.*), Phys. Rev. Lett. **100**, 112001 (2008).

96. CLEO Collaboration (M. Artuso *et al.*), Phys. Rev. Lett. **94**, 032001 (2005) hep-ex/0411068.

97. M.J. Galuska, undergraduate thesis submitted to the University of Giessen (2008) (in German).

98. A.M. Badalian, B.L.G. Bakker, I.V. Danilkin, Phys. Rev. D **79**, 037505 (2009) arXiv:0812.2136 [hep-ph].

99. A.M. Badalian, B.L.G. Bakker, I.V. Danilkin, Phys. At. Nucl. **73**, 138 (2010) arXiv:0903.3643 [hep-ph].

100. B. -QLi, K.-T. Chao, Commun. Theor. Phys. **52**, 653 (2009) arXiv:0909.1369 [hep-ph].

101. S. Godfrey, N. Isgur, Phys. Rev. D **32**, 189 (1985) S. Godfrey, R. Kokoski, **43**, 1679 (1991).

102. Y.S. Kalashnikova, A.V. Nefediev, Phys. Lett. B **530**, 117 (2002) hep-ph/0112330.

103. D. Ebert, V.O. Galkin, R.N. Faustov, Phys. Rev. D **57**, 5663 (1998).

104. W.A. Bardeen, E.J. Eichten, C.T. Hill, Phys. Rev. D **68**, 054024 (2003).

105. P. Colangelo, F. De Fazio, R. Ferrandes, Nucl. Phys. (Proc. Suppl.) **163**, 177 (2007).

106. A.F. Falk, T. Mehen, Phys. Rev. D **53**, 231 (1996).

107. R. Lewis, R.M. Woloshyn, Phys. Rev. D **62**, 114507 (2000).

108. L.M. Abreu, D. Cabrera, F.J. Llanes-Estrada, J.M. Torres-Rincon, Annals Phys. **326**, 2737 (2011) arXiv: 1104.3815 [hep-ph].

109. E.E. Kolomeitsev, M.F.M. Lutz, Phys. Lett. B **582**, 39 (2004) hep-ph/0307133.

110. J. Hofmann, M.F.M. Lutz, Nucl. Phys. A **733**, 142 (2004) hep-ph/0308263.

111. F.-K. Guo, P.-N. Shen, H.-C. Chiang, R.-G. Ping, B.-S. Zou, Phys. Lett. B **641**, 278 (2006) hep-ph/0603072.

112. F.-K. Guo, P.-N. Shen, H.-C. Chiang, Phys. Lett. B **647**, 133 (2007) hep-ph/0610008.

113. Belle Collaboration (K. Abe *et al.*), Phys. Rev. Lett. **98**, 082001 (2007) hep-ex/0507019.

114. S.P. Baranov, V.L. Slad, Phys. At. Nucl. **67**, 808 (2004) hep-ph/0603090.

115. J.D. Bjorken, *Is the CCC a New Deal for Baryon Spectroscopy?*, FERMILAB-CONF-85-069, C85-04-20 (1985).

116. Y.Q. Chen, S.Z. Wu, JHEP **08**, 144 (2011) **09**, 089(E) (2011) arXiv:1106.0193 [hep-ph].

117. N. Brambilla, J. Ghiglieri, A. Vairo, Phys. Rev. D **81**, 054031 (2010) arXiv:0911.3541 [hep-ph].

118. J.M. Flynn, E. Hernandez, J. Nieves, Phys. Rev. D **85**, 014012 (2012) arXiv:1110.2962 [hep-ph].

119. F.J. Llanes-Estrada, O.I. Pavlova, R. Williams, Eur. Phys. J. C **72**, 2019 (2012) arXiv:1111.7087 [hep-ph].

120. G.P. Lepage, S.J. Brodsky, Phys. Lett. B **87**, 359 (1979); Phys. Rev. D **22**, 2157 (1980).

121. S.J. Brodsky, G.R. Farrar, Phys. Rev. Lett. **31**, 1153 (1973).

122. J. Volmer *et al.*, Phys. Rev. Lett. **86**, 1713 (2001).

123. T. Horn *et al.*, Phys. Rev. Lett. **97**, 192001 (2006).

124. V. Tadevosyan *et al.*, Phys. Rev. C **75**, 055205 (2007).

125. M. Gorchtein, P. Guo, A.P. Szczepaniak, to be published in Phys. Rev. C arXiv:1102.5558 [nucl-th] and arXiv: 1106.5252 [hep-ph].

126. S. Noguera, V. Vento, Eur. Phys. J. A **48**, 143 (2012) arXiv:1205.4598 [hep-ph].

127. M. Diehl, T. Gousset, B. Pire, Phys. Rev. D **62**, 073014 (2000) hep-ph/0003233 M. Diehl *et al.*, Phys. Rev. Lett. **81**, 1782 (1998) [hep-ph/9805380].

128. A. Ahmed, arXiv:1106.0740 [hep-ph].

129. A.K. Leibovich, I.W. Stewart, Phys. Rev. D **57**, 5620 (1998) hep-ph/9711257.

130. Yu.A. Simonov, Phys. Rev. D **85**, 105025 (2012) arXiv: 1109.5545 [hep-ph].

131. R. Fleischer, D. Wyler, Phys. Rev. D **62**, 057503 (2000) hep-ph/0004010.

132. B. Meadows, M. Blanke, A. Stocchi, A. Drutskoy, A. Cervelli, M. Giorgi, A. Lusiani, A. Perez *et al.*, arXiv:1109.5028 [hep-ex].

133. J. Vijande, F. Fernandez, A. Valcarce, B. Silvestre-Brac, Eur. Phys. J. A **19**, 383 (2004) hep-ph/0310007.